91

SATELLITE & MESOMETEOROLOGY RESEARCH PROJECT

Department of the Geophysical Sciences
The University of Chicago
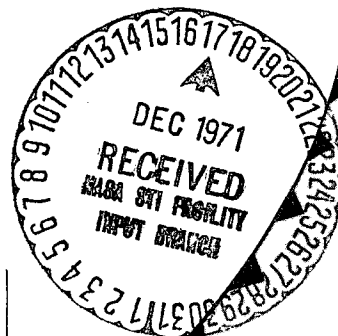
PROPOSED CHARACTERIZATION OF TORNADOES AND

HURRICANES BY AREA AND INTENSITY

by

T. Theodore Fujita

The University of Chicago

DEC 1971
RECEIVED
NASA STI FACILITY
INPUT BRANCH

FAC (NASA CR OR TMX OR AD NUMBER)

SMRP Research Paper

Number 91

February 1971

46 p.

Proposed Characterization of Tornadoes and
Hurricanes by Area and Intensity

by

T. Theodore Fujita
The University of Chicago

TABLE OF CONTENTS

Proposed Characterization of Tornadoes and
Hurricanes by Area and Intensity

by

T. Theodore Fujita
The University of Chicago

A B S T R A C T

Results of the 1968 through 1970 Tornado Watch Experiment conducted jointly by
NASA and NOAA suggested the necessity of characterizing individual tornadoes in order
to improve the identity of tornado-producing nephsystems. An attempt was made, there-
fore, to categorize each tornado by its intensity and area. Fujita-scale wind and corre-
sponding damage categories were devised to classify tornadoes as Gale (F0), Weak (F1),
Strong (F2), Severe (F3), Devastating (F4), and Incredible (F5). Additionally, indi-
vidual tornado areas were also categorized as Trace (TR), Decimicro (DM), Micro (MI),
Meso (ME), Macro (MA), Giant (GI), and Decagiant (DG), thus permitting us to charac-
terize a tornado by a combination of intensity and area, such as "Weak Decimicro Tor-
nado", "Severe Meso Tornado", "Incredible Giant Tornado", etc. A test characteriza-
tion of 156 Japanese tornadoes in 1950-69 was accomplished for comparison with 893 U.S.
tornadoes in 1965. Unexpectedly, the percentage distribution of intensity and individual
area of U.S. and Japanese tornadoes is very similar except for large and/or intense ones.
Intensity distribution within the Dallas and Fargo tornadoes of 1957 was also studied in
detail. It was also found that the F-scale variation along the paths of family tornadoes
shows an intensity oscillation with a 45-min interval. For further applications, charac-
terization of Atlantic hurricanes, Pacific hurricanes, and Pacific typhoons was made to
determine the trend of their cumulative frequencies. It was found that 90% of these
storms are characterized, in each region respectively, by less than F2.8, F2.3, and
F3.3, indicating clearly that average typhoons are more intense than average hurricanes.
Finally, the areas of Hurricane Camille of August 1969 and the Ise-wan typhoon of
September 1959 are analyzed with F-scale contours in an attempt to determine the distri-
bution of damaging winds within these storms.

1. INTRODUCTION

During a three-year period, 1968-1970, annual tornado watch experiments were conducted under the sponsorship of NASA and NOAA in an attempt to investigate satellite-viewed cloud characteristics in relation to tornado occurrences. The evaluation of tornado and nephsystem relationship turned out to be rather inconclusive because those storms reported as tornadoes are not always large and intense, destroying only weak structures during their few-minute life time. Some storms are, on the other hand, long lived with their incredible intensity resulting in total destruction of even steel structures.

In an attempt to improve our basic understanding of tornado-producing thunderstorms viewed from geostationary satellites, past tornado data based on storm data and other sources were reexamined so as to classify individual storms according to their intensity as well as their affected area.

The frequency of reported tornadoes since 1916, when systematic tabulation began, has been increasing during the past half century although the frequencies in the 1960s leveled off to a certain extent. Such a trend is shown clearly in statistical papers by Wolford (1960), Thom (1963), Pautz (1969), and Court (1970). The importance of mean duration in relation to mean length of travel was emphasized by Battan (1959) who derived the mean duration as less than 2 minutes. For the assessment of tornado probability at given points in the United States, the mean area of tornadoes is of vital importance. The mean area was not well known until Thom (1963) estimated the mean area to be 2.8 sq. miles. Such an estimate is absolutely necessary to compute tornado probabilities since the larger the mean area the higher the damage probability even if the total frequency of tornadoes remains unchanged.

An attempt to categorize tornadoes, all if possible, was made by Fujita (1970) who used those recorded in Storm Data for 1965, 1967, and 1969 with reported lengths and widths. Analysis of 793 tornadoes in these three years revealed that the individual tornado areas obtained by simply multiplying the length by the width recorded in Storm Data vary through 6 orders of magnitude from 0.001 to 100 sq. miles.

Tornado intensity is much harder to estimate than tornado affected area because the extent of damage to structures and trees cannot as easily be expressed numerically. By examining damage descriptions in Storm Data, it was felt first that a reasonable scale of damage can be established if an educated guess is made. The Chicago tornado of

2

March 4, 1961, studied by Brown and Fujita (1961), should be rated as much weaker than the Dallas tornado of April 2, 1957 which was, however, considerably weaker than the Fargo tornado of June 20, 1957. The author made a detailed aerial survey of 25 Palm Sunday tornadoes of April 11, 1970 and found that none of the 25 was as intense as the Fargo tornado, despite the fact that it was a day of tremendous outbreak of large and intense storms. When the author surveyed the Lubbock tornado of May 11, 1970, Fargo-type, intense damage was found in many parts of the damage area. Thus, the feasibility of characterizing Chicago to Lubbock type tornadoes into 3 or 4 categories appears to be realistic. By adding one or two weaker categories below the Chicago tornado category, it would be a logical attempt to differentiate damage caused by 50 to about 300-mph winds into 5 to 6 categories through an educated guess by means of the characterization method described in the following paragraphs.

2. PROPOSED SCALE OF DAMAGING WIND

Although the frequency of tornadoes in the midwestern United States is the highest in the world, the probability of observing a tornado from a fixed location is slightly higher than once in a century. A chance that a wind recorder happens to be in the immediate vicinity of a passing tornado is extremely rare. Moreover, most wind instruments are not designed to record wind speeds in excess of 150 mph and their survival in much higher wind speeds is unlikely.

Wind speeds in tornadoes have been estimated from structural damage, characteristic ground marks, scanning and scaling motion pictures, and the shape of funnel clouds. Each of these estimates requires weeks of time in order to achieve the highest possible accuracy. On the other hand, one may be able to make extremely rough estimates of wind-speed ranges through on-the-spot inspection of storm damage. For instance, the patterns of damage caused by 50 and 250-mph winds are so different that even a casual observer can recognize the differences immediately. The logic involved is that the higher the estimate accuracy the longer the time required to make the estimate. Thus, a few weeks of time necessary for an estimate with a 5-mph accuracy can be reduced drastically to a few seconds if only a 100 mph accuracy is permissible in order to obtain a large number of estimates with considerably less accuracies. An important compromise is to make an educated guess of the speed ranges by inspecting either actual damage or aerial

photographs taken after a storm. A survey of the literature reporting the results of time-consuming, accurate estimates implies that 30-mph increments within relatively low wind-speed ranges and 50-mph increments within rather high wind-speed ranges result in characteristic damage patterns which can be distinguished by trained individuals with the help of damage specifications similar to those used in estimating the Beaufort wind forces by trained observers. Only a few seconds will be required to perform such an educated guess. An existing Beaufort wind force extended beyond B 12 is too small a speed increment to distinguish damage corresponding to one force or another.

The proposed scale of damaging wind is designed to connect smoothly the Beaufort force, B 12, with the speed of sound in the atmosphere or Mach number, M1. This scale which may be called F scale corresponds to Beaufort force and Mach number at the following wind speeds.

$$F 1 \ = \text{Beaufort } 12$$
$$\text{and} \quad F 12 = \text{Mach } 1 \quad \text{at} \quad -3^\circ C.$$

Equations for computing B, F, and M wind speeds are:

$$V \ = \ 0.836 \ B^{\frac{3}{2}} \ (\text{m/sec}) \ = \ 1.870 \ B^{\frac{3}{2}} \ (\text{mph}) \tag{1}$$

$$V \ = \ 6.30 \ (F + 2)^{\frac{3}{2}} \ (\text{m/sec}) \ = \ 14.1 \ (F + 2)^{\frac{3}{2}} \ (\text{mph}) \tag{2}$$

$$V \ = \ (331 + 0.6 t) M \ (\text{m/sec}) \ = \ (742 + 1.3 t) M \ (\text{mph}) \tag{3}$$

where B, F, and M are, respectively, Beaufort force, Fujita scale, and Mach number, V the corresponding wind speed, and t, the air temperature in $^\circ$ C.

In deriving Eq. (2) for F scale wind computation, a linear formula such as for Mach number was avoided because it is desirable to have a small speed increment when speed is relatively low. In obtaining such a speed range, $(F + 2)^{\frac{3}{2}}$ was introduced. This simple function has three advantages: (a) the square of the speed or the energy is proportional to the cube of $(F + 2)$, (b) the speed corresponding to $F = 0$ represents a finite value of 40 mph which would cause little damage on most structures, and (c) the speed ranges between F 0 and F 1, F 1 and F 2, etc. increases 33, 40, 45, 49 mph, etc., resulting in distinguishable speed ranges increasing with F numbers.

Due to the fact that F-scale winds are estimated from structural and/or tree damage, the estimated wind speed applies to the height of the apparent damage above the ground. In addition to the speed and the height of damaging wind, duration is also of vital importance to the yielding point of a structure. While disregarding the gust period and amplitude at this moment, the period of sustained wind must be specified. Internationally, ten-minute average values are used in synoptic reports, while one-minute average values are used in the United States. A station equipped with a multiple register determines the fastest speed in miles per hour of any "mile" wind. At 60 mph, the fastest-mile wind speed and one-minute mean speed are identical.

In connection with definitions of one-minute average, 10-minute average, and the fastest mile winds, it would be necessary to clarify the definition of the F scale wind speed computed from Eq. (2). A 10-min period or even a one-minute period wind seems to be too long to be required to destroy a structure or to blow down a tree. The period of a sustained wind required to complete a damage is likely to be inversely proportional to the wind speed, suggesting strongly that damaging wind must be defined as the fastest "wind path length" rather than the average speed during a sustained wind period. When the wind path length is selected to be "one mile", we call the wind the fastest mile wind. In reality, however, only a fraction of one mile would be required to complete a destruction of trees and structures. F-scale wind speed in this paper was thus defined to be the "fastest 1/4 mile wind". For F 4 wind speed of about 200 mph, the duration of the damaging wind would be only about 4 seconds.

Damaging wind speeds in mph, knots, and m/sec together with the periods of the fastest 1/4 mile winds are presented in Table I. Note that F 1.0 corresponds to 73 mph, the beginning of hurricane wind. In view of possible occurrences of light damage when F is larger than 0.0 or 40 mph, the table was made to include F 0.0 and higher speeds. Under the presumption that the occurrences of F 6 or higher wind are extremely rare, wind speeds above F 6 are tabulated for the range of each full scale, F 7, F 8, etc. Presented also in the table are damage categories to be expected by F 0 through F 5 winds.

In addition to the speed ranges corresponding to F 0, F 1, F 2, etc. , the table includes the fractional F scales such as F 1.3, F 2.8, etc. These values do not imply that the fractional F scales can be estimated through visual inspections of damage. The fractional F scales can be computed only from anemometer record or engineering

5

Table I. TABLE OF FUJITA SCALE DAMAGING WIND SPEED
F-scale wind speed is defined as the fastest ¼-mile wind at the
height of damaged structure of object. The last column indicates
the period of the fastest ¼-mile wind in seconds.

F 0	(40 - 72 mph)	Light Damage
F 1	(73 - 112 mph)	Moderate Damage
F 2	(113 - 157 mph)	Considerable Damage
F 3	(158 - 206 mph)	Severe Damage
F 4	(207 - 260 mph)	Devastating Damage
F 5	(261 - 318 mph)	Incredible Damage

F-scale	mph	knots	m/sec	Period
F 0.0 - 0.1	40 - 45	35 - 39	17.8 - 20.5	22.5 - 19.6
0.2 - 0.3	46 - 51	40 - 45	20.6 - 23.3	19.5 - 17.2
0.4 - 0.5	52 - 58	46 - 50	23.4 - 26.3	17.1 - 15.3
0.6 - 0.7	59 - 65	51 - 56	26.4 - 29.4	15.2 - 13.7
0.8 - 0.9	66 - 72	57 - 63	29.5 - 32.6	13.6 - 12.3
F 1.0 - 1.1	73 - 80	64 - 69	32.7 - 36.0	12.2 - 11.2
1.2 - 1.3	81 - 87	70 - 76	36.1 - 39.4	11.1 - 10.2
1.4 - 1.5	88 - 95	77 - 83	39.5 - 42.9	10.1 - 9.4
1.6 - 1.7	96 - 103	84 - 90	43.0 - 46.6	9.3 - 8.7
1.8 - 1.9	104 - 112	91 - 97	46.7 - 50.3	8.6 - 8.1
F 2.0 - 2.1	113 - 120	98 - 104	50.4 - 54.1	8.0 - 7.5
2.2 - 2.3	121 - 129	105 - 112	54.2 - 58.1	7.4 - 7.0
2.4 - 2.5	130 - 138	113 - 120	58.2 - 62.1	6.9 - 6.5
2.6 - 2.7	139 - 147	121 - 128	62.2 - 66.2	6.4 - 6.2
2.8 - 2.9	148 - 157	129 - 136	66.3 - 70.3	6.1 - 5.8
F 3.0 - 3.1	158 - 166	137 - 144	70.4 - 74.6	5.7 - 5.5
3.2 - 3.3	167 - 176	145 - 153	74.7 - 79.0	5.4 - 5.2
3.4 - 3.5	177 - 186	154 - 161	79.1 - 83.4	5.1 - 4.9
3.6 - 3.7	187 - 196	162 - 170	83.5 - 87.9	4.8 - 4.7
3.8 - 3.9	197 - 206	171 - 179	88.0 - 92.5	4.6 - 4.4
F 4.0 - 4.1	207 - 217	180 - 188	92.6 - 97.2	4.3 - 4.2
4.2 - 4.3	218 - 227	189 - 197	97.3 - 101.9	4.1 - 4.0
4.4 - 4.5	228 - 238	198 - 207	102.0 - 106.7	3.9
4.6 - 4.7	239 - 249	208 - 216	106.8 - 111.6	3.8 - 3.7
4.8 - 4.9	250 - 260	217 - 226	111.7 - 116.6	3.6 - 3.5
F 5.0 - 5.1	261 - 271	227 - 235	116.7 - 121.6	3.4
5.2 - 5.3	272 - 283	236 - 245	121.7 - 126.7	3.3
5.4 - 5.5	284 - 294	246 - 255	126.8 - 131.9	3.2 - 3.1
5.6 - 5.7	295 - 306	256 - 266	132.0 - 137.1	3.0
5.8 - 5.9	307 - 318	267 - 276	137.2 - 142.5	2.9
F 6.0 - 6.9	319 - 380	277 - 329	142.6 - 170.0	2.8 - 2.5
F 7.0 - 7.9	381 - 445	330 - 386	170.1 - 199.1	2.4 - 2.1
F 8.0 - 8.9	446 - 513	387 - 446	199.2 - 229.7	2.0 - 1.8
F 9.0 - 9.9	514 - 585	447 - 508	229.8 - 261.8	1.7 - 1.6
F10.0 - 10.9	586 - 660	509 - 573	261.9 - 295.2	1.5
F11.0 - 11.9	661 - 737	574 - 640	295.3 - 329.9	1.4 - 1.3
F12.0 - 12.9	738 - 818	641 - 710	330.0 - 365.9	1.2 - 1.1

estimates of storm damage.

Figure 1 was prepared to show the connection of Beaufort force, Fujita Scale and Mach number. According to the summary prepared by List (1958), Beaufort forces are numerically extended to B17 (131 mph) which corresponds to F2.4. By extending the F-scale wind speed downward below F1.0, it is seen that the curve ends at wind speed zero corresponding to F = -2. Mach number wind speed for a given air temperature is expressed by a straight line on which fractional Mach numbers such as 0.6, 0.7, ... are indicated.
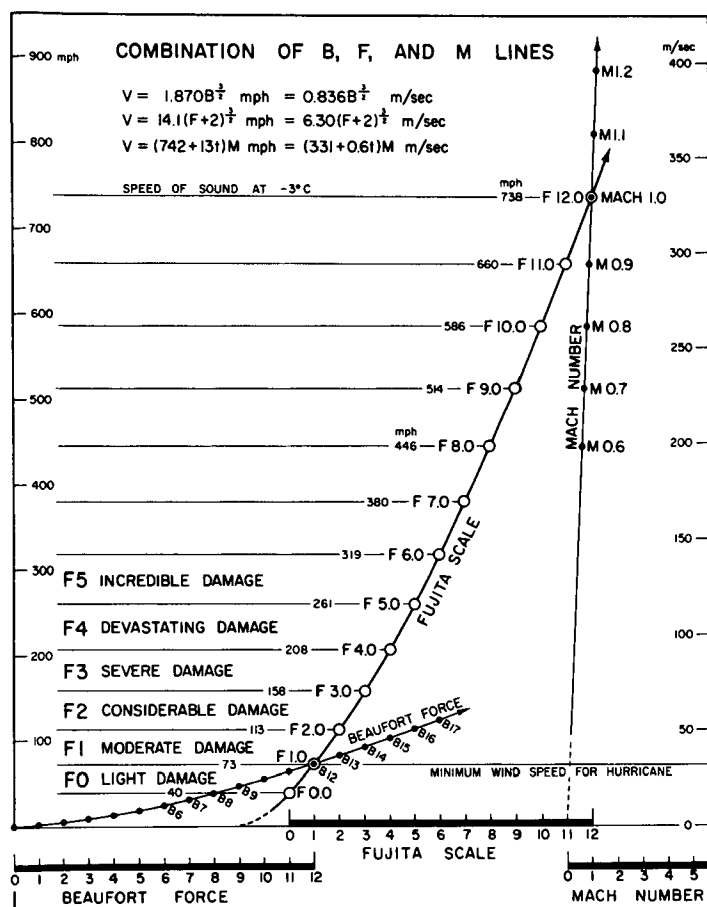
Fig. 1. Connection of Beaufort force, Fujita scale and Mach number. In deriving the equation for F-scale wind computation, the following considerations were made. (1) To connect Beaufort force 12 with Mach number 1 with a smooth curve, (2) To correspond B 12 with F 1 and M 1 with F 12, so that a 1 through 12 graduated scale, as in the case Beaufort force, covers the desired speed range. (3) Beaufort 0 indicates calm or no wind and Fujita 0 likewise denotes the wind speed causing no damage on most structures, (4) To give wider speed range as the speed increases because the faster the wind speed the wider the speed range to allow a visual distinction of damage from one scale to the next, and (5) An exponent 3/2 is likely to serve the above purpose. Furthermore, the square of the speed or the kinetic energy is proportional to the cube of F + 2. About 20 formulas to satisfy partial or total conditions listed above were examined before adopting Eq (2), the final equation, which was used to obtain the F-scale curve presented in this figure.

3. SPECIFICATION OF DAMAGE CORRESPONDING TO F-SCALE WIND SPEEDS

F-scale wind speeds introduced in the previous section are nothing but the speeds computed from Eq. (2) which was formulated to connect Beaufort force with Mach number. It is then necessary to obtain damage specifications corresponding to each F scale. Since no direct measurements of wind speed inside tornadoes are available, various estimates

of wind speeds and corresponding damage characteristics were studied in detail.

Early estimates of the highest tornado wind speed reported by Flora (1954) and some others are as high as 500 mph. Engineering estimates revealed, however, that up to 350 mph winds lasting a few seconds are likely to produce most tornado damage in the Midwest. A comprehensive summary of tornado wind speeds based on various methods was completed by Melaragno (1968) in an attempt to assess tornado forces and their effects on buildings.

Australian tornadoes were summarized by Clarke (1962). He stated that the "Brighton tornado", Melbourne, February 2, 1918, which severely damaged well-constructed buildings was accompanied by an estimated 200-mph wind which was the highest estimated speed in Australia. Clarke indicated that 98% of Australian tornadoes are characterized by winds less than 120 mph and 72% by winds less than 73 mph which corresponds to the Beaufort 12 or F1 scale.

Based on these estimated speeds along with a large number of aerial and ground photographs of tornado damage, F0 through F5 damage specifications were obtained.

FUJITA SCALE DAMAGE SPECIFICATIONS

(F 0) 40 - 72 mph, LIGHT DAMAGE

Some damage to chimneys and TV antennae; breaks twigs off trees; pushes over shallow rooted trees.

(F 1) 73 - 112 mph, MODERATE DAMAGE

Peels surface off roofs; windows broken; light trailer houses pushed or overturned; some trees uprooted or snapped; moving automobiles pushed off the road. 73 mph is the beginning of hurricane wind speed.

(F 2) 113 - 157 mph, CONSIDERABLE DAMAGE

Roofs torn off frame houses leaving strong upright walls; weak buildings in rural areas demolished; trailer houses destroyed; large trees snapped or uprooted; railroad boxcars pushed over; light object missiles generated; cars blown off highway.

(F 3)   158 - 206 mph, SEVERE DAMAGE

Roofs and some walls torn off frame houses; some rural buildings completely demolished; trains overturned; steel-framed hangar-warehouse type structures torn; cars lifted off the ground; most trees in a forest uprooted, snapped, or leveled.

(F 4)   207 - 260 mph, DEVASTATING DAMAGE

Whole frame houses leveled, leaving piles of debris; steel structures badly damaged; trees debarked by small flying debris; cars and trains thrown some distances or rolled considerable distances; large missiles generated.

(F 5)   261 - 318 mph, INCREDIBLE DAMAGE

Whole frame houses tossed off foundations; steel-reinforced concrete structures badly damaged; automobile-sized missiles generated; incredible phenomena can occur.

(F6-12)   319 mph to sonic speed, INCONCEIVABLE DAMAGE

Should a tornado with the maximum wind speed in excess of F 6 occur, the extent and types of damage may not be conceived. A number of missiles such as ice boxes, water heaters, storage tanks, automobiles, etc. will create serious secondary damage on structures.

The above damage specifications were based mostly on engineering estimates of wind speeds, involving both drag and lift forces which are assumed to be proportional to the square of the wind speed. As shown in the schematic outline of a house in Fig. 2, a straight flow impinging against a house creates a positive pressure on the upwind wall A. Due to the acceleration of the flow around the corners, a significant negative dynamic pressure is created at B, C, and D. Negative dynamic pressure on the roof is usually
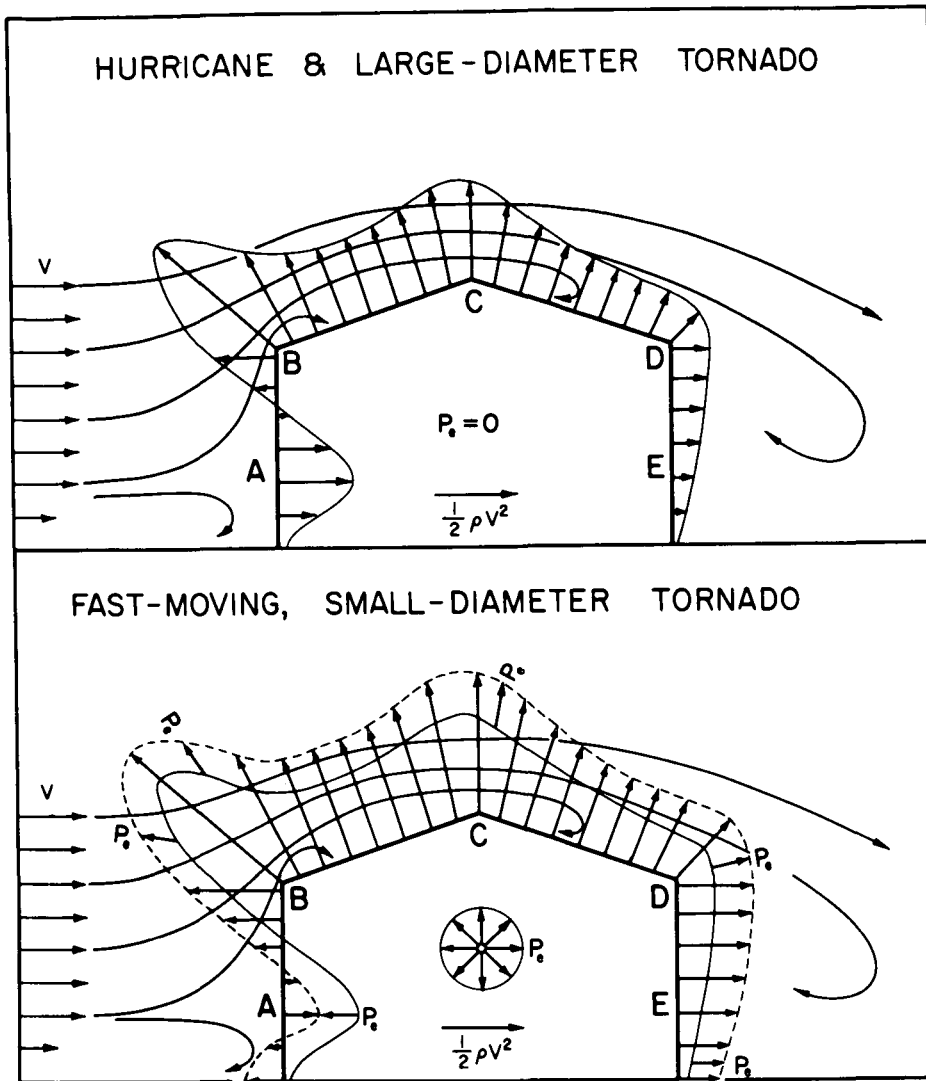
Fig. 2. Schematic flow patterns and induced dynamic pressure around a house standing in tornadic wind. Note that the reduction of pressure by a passing tornado as a whole acts as an explosive pressure superimposed upon the wind-induced dynamic pressure.

more significant than on walls, resulting in the peeling of roofing materials or removal of the roof without damaging upright walls. Thus a portion of the debris from a house can be found even on the upwind side of standing walls. If the speed of damaging wind exceeds that of F 3, walls start collapsing. With F 5 or higher wind, the drag force is so large that all walls of a frame house can be torn from the foundation and the lift force creates a flying house.

A fast-moving tornado with a relatively small core diameter creates an additional pressure reduction problem. If a house is air tight, the hydrostatic reduction of pressure due to an approaching tornado increases the in-house pressure relative to the outside pressure. This pressure which may be called the "explosive pressure", P_e , will be considerably reduced when a house is properly vented, especially on the downwind

DAMAGING WIND SCALE BY FUJITA

Scale	m / sec	Knots	mph	Expected Damage
F 0	17.8- 32.6	35- 63	40- 72	LIGHT DAMAGE
F 1	32.7- 50.3	64- 97	73-112	MODERATE DAMAGE
F 2	50.4- 70.3	98-136	113-157	CONSIDERABLE DAMAGE
F 3	70.4- 91.9	137-179	158-206	SEVERE DAMAGE
F 4	92.0-116.6	180-226	207-260	DEVASTATING DAMAGE
F 5	116.7-142.5	227-276	261-318	INCREDIBLE DAMAGE

From SMRP Research Paper Number 91.
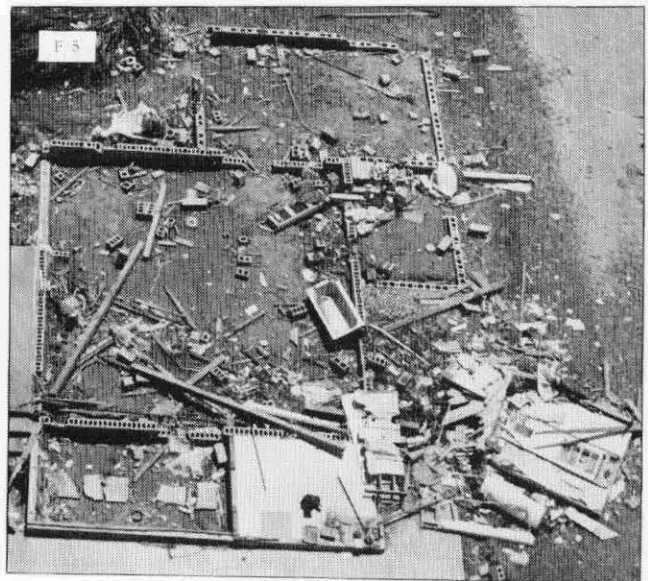
Fig. 3. F-scale damage chart applicable to relatively new suburban structures. Damage scenes were selected from color pictures of Lubbock tornado, May 11, 1970, taken by the author from about 500-ft altitude.

11

side. Although the amount of P_e which depends upon the translational speed and the pressure profile of the storm as well as the venting mode of a structure, cannot be estimated for each damage case, the explosive pressure does accelerate the roof removal or house explosion for a given range of F-scale wind speeds. As a result, one could overestimate an F scale by one. Such an overestimation can be avoided, however, by examining nearby structures and trees especially when an exploded house is surrounded by undamaged or slightly damaged structures.

To aid F-scale determinations from damage specifications, the damage chart of Fig. 3 was prepared. This chart is applicable to most suburban structures with block foundations and walls and relatively weak roofing. No damage scene for F0 is included in the chart because the damage is insignificant in aerial pictures. It is seen in the F1 scene that some to most roofing materials are peeled off frame houses. The F2 scene shows a typical aerial view of a house with its torn roof and standing upright walls. Since the Lubbock tornado of May 11, 1970, with an extremely large core diameter, was moving slowly when this damage occurred, the roof was torn mostly by wind-induced dynamic pressure similar to that experienced in intense hurricanes. As shown in the F3 scene, some upright walls were torn from a motel building; individual block-sized missiles were found stuck in ground-floor walls. The F4 scene shows a leveled structure with all items except the foundation dislocated from their original positions. Trees around this building were debarked by small flying debris which are usually captured by tree trunks at low wind speeds. The F5 scene taken in the northern suburb of Lubbock clearly shows the foundation of a house which had sailed away toward the lower right, leaving behind a water heater and a bath tub. All trees around the house were flattened, losing most of the bark from their trunks.

4. APPLICATION OF F SCALE IN TORNADO ANALYSES

Damage charts and specifications introduced in the previous chapter can now be used in determining F-scale variations along the paths of well-documented storms.

Investigations of the Dallas tornado of April 2, 1957 by Hoecker (1960a) (1960b), Beebe (1960), and Segner (1960) were used to produce the life history chart of Fig. 4. The top graph was constructed by plotting as a function of time the heights of the funnel appearing in Hoecker's (1960a) 57 sketches. These sketches were used to determine the

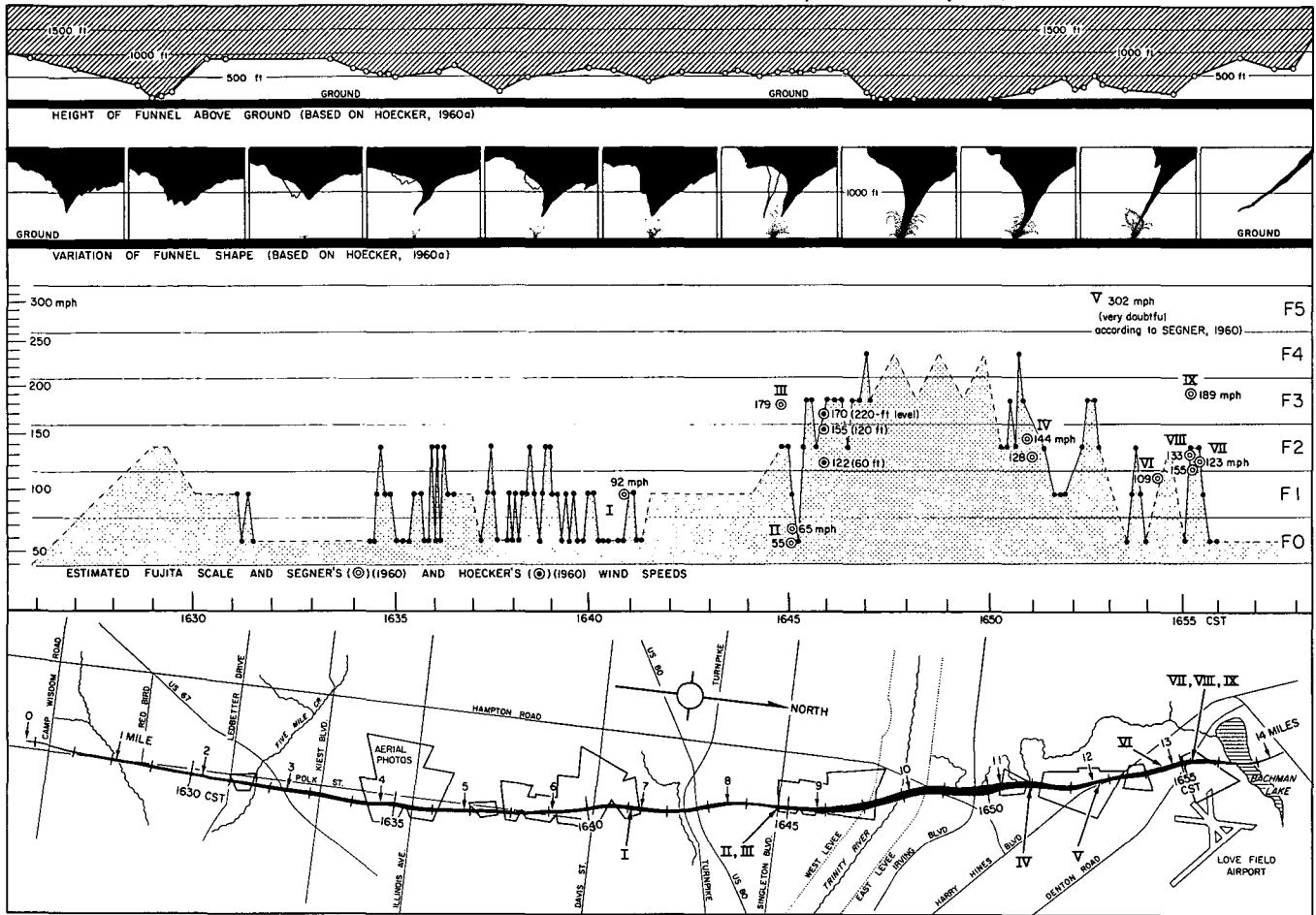# LIFE HISTORY OF DALLAS TORNADO, APRIL 2, 1957

Fig. 4. Life history of Dallas tornado of April 2, 1957 as depicted by the height and shape of the funnel, variation of F-scale damage, and the estimated wind speeds along the tornado path.

Fig. 5. Life history of Fargo tornado of June 20, 1957. Note that this storm was larger and more intense than Dallas tornado in Fig. 4.

schematic variation of the funnel. Shown in the bottom chart in the figure is the tornado path with areas covered by aerial photos appearing in Beebe's (1960) analysis. The locations of engineering estimates by Segner (1960) are identified by Roman numerals, I, II, III, etc. The middle diagram shows the variation of F-scale damage estimated by the author based on aerial photographs. Despite the fact that the F scale varies practically from house to house, one must accept such variations as the built-in noise superimposed upon overall patterns of tornado damage. Segner's estimated values ranging between 55 and 189 mph (one 302 mph value which he stated doubtful) seem to fit the F-scale variations determined from aerial photographs. These test analyses suggest that it would be highly desirable to determine house-to-house variation of F-scale intensity in order to interpret properly the time-consuming engineering estimates of maximum and/or minimum wind speeds causing specific damage.

A similar life history chart of the Fargo tornado of June 20, 1957 (see Fig. 5) was constructed based on the storm analysis by Fujita (1960). The Fargo tornado funnel was a giant compared to the Dallas tornado. When the funnel was on the ground, the storm caused F5 damage between 25th and 29th Streets shown in the bottom chart. At that time, the funnel diameter on the ground was estimated to be about 500 ft. Thereafter, the funnel was lifted 4 to 500 ft above the ground, but the damage scale beneath the lifted funnel varied between F1 and 3, suggesting that the damaging wind at the building levels was between 75 and 200 mph. As shown in the middle chart, the rotation rate of the funnel shortly after its formation was 107 mph. By adding a 35-mph translational speed of the tornado, the combined speed at the funnel level should be 142 mph. The wind speed affecting the building beneath the funnel is likely to be smaller than this value.

5. APPLICATION OF ESTIMATED F SCALES FOR PERIODIC INTENSIFICATION
   OF FAMILY TORNADOES

It has been known that tornadoes often spawn from a parent cloud in the form of a family. Fujita (1963) pointed out that the average occurrence interval is about 45 minutes. Darkow and Ross (1970) studied 7 parent storms in Missouri, 1964 through 1968, obtaining average occurrence intervals of 45 min. As shown in Table II, the intervals are mostly independent of the storms traveling speed ranging between 15 and 62 mph.

15

| Date of Tornado	Tornado Identification		Path Length	Tornado Duration	Occurrence Interval	Speed of Parent Storm
27 June 1955	Scottsbluff	#1	8 miles	? min	38 min	15 mph
		#2	4	29	42	
		#3	9	45		
20 June 1957	Fargo	#1	11 miles	45 min	40 min	19 mph
		#2	7	35	42	
		#3	8	63	43	
		#4	10	35	40	
		#5	7	25		
2 April 1957	Dallas	#1	14 miles	35 min	27 min	26 mph
		#2	3+	?		
9 June 1953	Worcester	#1	45 miles	75 min	65 min	30 mph
		#2	29	65		
25 May 1955	Blackwell	#1	39 miles	60 min	40 min	31 mph
		#2	37	50		
11 April 1965	Bi-state	#1	21 miles	20 min	23 min	62 mph
		#2	51	49	49	
		#3	58	56	64	
		#4	38	37	57	
		#5	18	17	46	
		#6	24	23		
Average of all storms			22.1 miles	42.5 min	44.0 min	30.5 mph
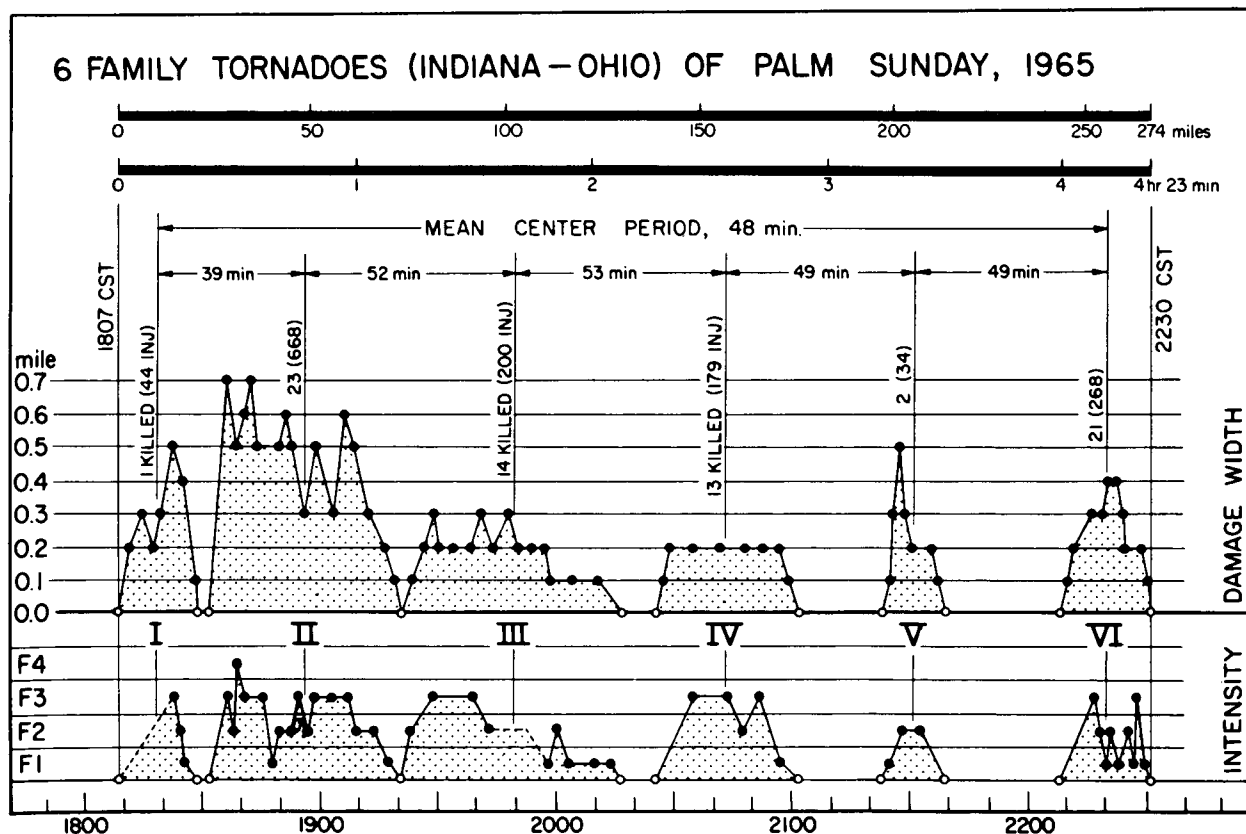
Fig. 6. Variation of damage width and F scale along the bi-state tornado of Palm Sunday, 1965. This storm, leaving a straight-line damage path of 274 miles from south of Lafayette, Ind. to Cleveland, Ohio, clearly shows 6 maxima in both damage width and storm intensity.

The proposed F-scale intensity of tornadoes when applied to a series of family tornadoes will permit us to describe the variation of the intensity as a function of either time or space. An example of 6 family tornadoes on Palm Sunday, 1965 is shown in Fig. 6. Note that F-scale intensity dropped down below F1 five times during the storm's 274 mile path in 4 hr 23 min. During this period the times when no damaging winds were on the ground were no longer than 30 minutes. The figure shows that the damage width or the diameter of damaging wind also changed periodically in phase with the storm's intensity. This is against the original expectation that the intensification will take place when the storm's diameter shrinks. Although the reasons for such an in-phase variation of the intensity and the damage diameter have not been solved, research is in progress to determine the time variation of the circulation around family tornadoes expressed as

$$\frac{d\Gamma}{dt} = \frac{d}{dt} \int_C V_t \, d\ell \tag{4}$$

where Γ denotes the circulation; V_t, the tangential velocity around a closed circuit C; and $d\ell$ the circuit element around the storm.

6. RANGES OF INDIVIDUAL TORNADO AREA

For the purpose of making the maximum use of Storm Data, as was done by Battan (1959), Thom (1963), and others, both lengths and widths of individual tornadoes were investigated closely. The individual tornado areas defined by Fujita (1970) and applied to each tornado recorded in Storm Data are found to vary through an extremely wide range such that the area ratio between the largest and the smallest exceeds 1,000,000 to 1. The author, therefore, tried to classify tornadoes according to their areas as shown in Table III. It is very unlikely that a tornado with its individual area in excess of 1000 sq. miles ever occurred in the past. The term HG (hectogiant) is, therefore, not included in the table. The accuracy of area estimates depends entirely upon the values given in Storm Data. Quoting Battan's (1959) statement, "Interviews with witness and damage surveys should pay particular attention to establishing the path length and duration of individual tornado funnels", the author, as one of the users of Storm Data, also wishes to stress the importance of the original data given in Storm Data for basic and applied research on tornadoes.

17

Table III. Classification of tornadoes according to individual areas defined by $a = L \times \bar{w}$ where L and $\bar{w}$ are the length and the mean width given in Storm Data.

Area Category		a in sq. mile			$\log a$
TR	(trace)	0	$< a <$	0.001	$\log a < -3$
DM	(decimicro)	0.001	$\leq a <$	0.01	$-3 \leq \log a < -2$
MI	(micro)	0.01	$\leq a <$	0.1	$-2 \leq \log a < -1$
ME	(meso)	0.1	$\leq a <$	1	$-1 \leq \log a < 0$
MA	(macro)	1	$\leq a <$	10	$0 \leq \log a < +1$
GI	(giant)	10	$\leq a <$	100	$1 \leq \log a < +2$
DG	(decagiant)	100	$\leq a <$	1000	$2 \leq \log a < +3$

As specified in Table II, the variation of the individual tornado area from one area category to the next is a factor of 10, meaning that relatively inaccurate estimates will still allow the selection of the most reasonable category.

7. CHARACTERIZATION OF TORNADOES BY AREA AND INTENSITY

Estimation of both tornado intensity and area by F-scale intensity and $\log a$ scale area is an initial improvement over merely counting the number of tornadoes, each of which is identified as a unit tornado. An attempt was made in this paper to "characterize" tornadoes based on these two parameters. Ideally, each storm should also be characterized by three-dimensional meteorological parameters such as temperature, humidity, pressure, wind, as well as funnel size, shape, duration, etc. It will be years before we are able to measure these meteorological parameters and their time changes accurately. The term "characterization" is used in this paper to express specific storm characteristics.

As a test characterization of tornadoes, Palm Sunday storms were selected because the author took a large number of aerial photographs to complete a report by Fujita, Bradbury, and Van Thullenar (1970). Since tornado characterization was not of primary significance when the initial studies were completed, all aerial photographs and notes were reexamined to establish both intensity and area classifications of the 25 major

storms for this day that were surveyed by the author. For unsurveyed storms, Storm Data were examined with the help of topographical maps to determine the most reasonable F and log σ scales. After extending the characterizations to include April 10, the pre-Palm Sunday storm day, the frequencies of occurrence belonging to each intensity and area were plotted as a function of the initial time of tornado occurrences (see Fig. 7). This figure clearly shows that the center of gravity of frequencies moved from F 1 on April 10 to F 2 on the 11th, suggesting that Mother Nature does produce intense tornadoes without increasing simultaneously the number of small ones. This means that the formation of an intense tornado is not the result of an accidental growth out of an increased number of small ones. Apparently, differing meteorological conditions produce tornadoes of differing intensity and area. Similarly the center of gravity in the Meso category on the 10th shifted to that of Macro on Palm Sunday. Note that Macro-sized tornadoes formed literally one after another between 12 noon and midnight.

In order to learn more about the distribution of tornado area and intensity, Tecson (1971), made a test analysis of 893 tornadoes in 1965 based on the storm description given in Storm Data. His results revealed that 77% of these tornadoes are in F 0 and F 1 categories while F 3 and F 4 storms are only 5% and 1%, respectively, of the total numbers, revealing that the frequency of intense tornadoes is very small.

When a similar analysis of Japanese tornadoes was made based on Japanese Storm Data (1950-69) 80% turned out to be in F 0 and F 1 categories while 3% were F 3. There were no reports of F 4 or higher categories. These results when examined along with U. S. data, as shown in Fig. 8, revealed that the distribution of F0, F 1, and F 2 of Japanese and U. S. tornadoes are very similar to each other. The real difference is the fact that F 4 and more intense storms occur in the U. S. but not in Japan.

Significant differences are also found in the frequency distribution of macro, giant, and decagiant categories which are practically non-existent in Japan. These storms are most likely to develop under very specific meteorological conditions experienced exclusively in the midwestern United States. In a recent five year period, the number of tornadoes reported in Japanese Storm Data was 13 (273) in 1965, 15 (315) 1966, 7 (147) 1967, 13 (273) 1968, and 15 (315) in 1969. Numbers in parenthesis indicate frequencies prorated to the U. S. area which is 21 times larger. These prorated frequencies are comparable to U. S. frequencies in 1951-52 when tornado frequencies began to increase

APR 10 (PRE-PALM SUNDAY), 1965 | **APR 11 (PALM SUNDAY), 1965**

6 am to 6 am TORNADO DAY — 6 am to 6 am TORNADO DAY

INTENSITY: INCREDIBLE, DEVASTATING, SEVERE, CONSIDERABLE, MODERATE, LIGHT — F5, F4, F3, F2, F1, F0

INDIVIDUAL AREA: DECAGIANT, GIANT, MACRO, MESO, MICRO, DECIMICRO, TRACE — DG, GI, MA, ME, MI, DM, TR
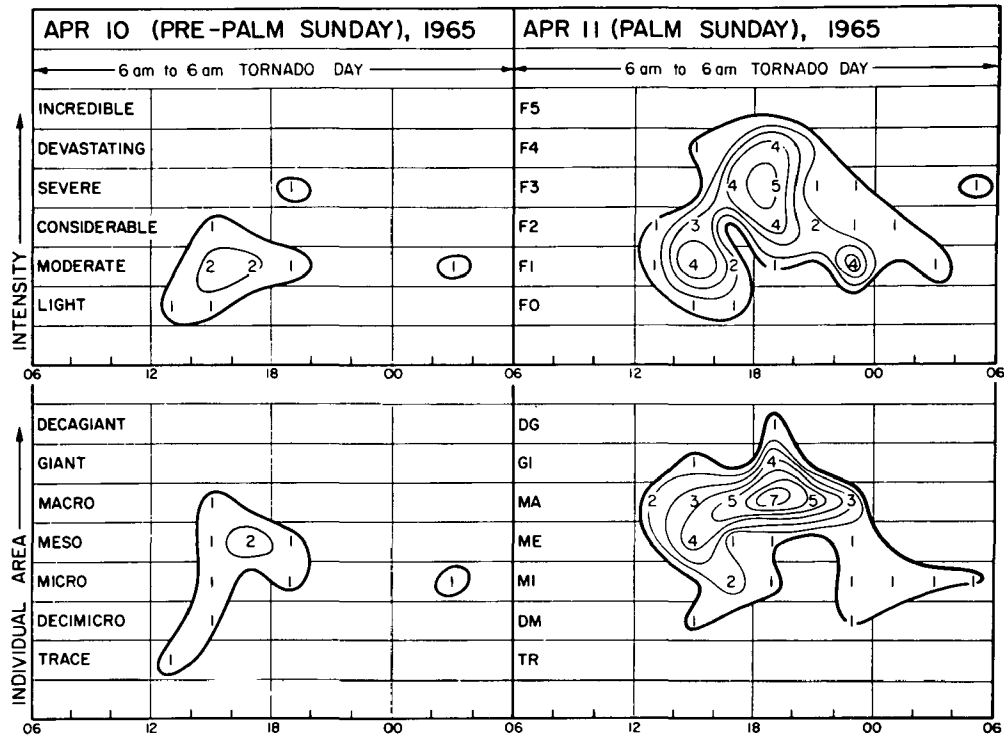
Fig. 7. Intensity and area distribution of pre- and Palm Sunday tornadoes of 1965. The numbers indicate the frequencies of characterized tornadoes within 2-hour period of each tornado day defined as a 24-hour period from 6 a.m. to 6 p.m. This definition of tornado day is reasonable especially when the tail end of tornado activity extends to early in the morning.

FREQUENCY OF TORNADOES BY INDIVIDUAL AREA AND INTENSITY

JAPAN	UNITED STATES	PALM SUNDAY
20 years (1950-69)	One year (1965)	One day (11 Apr 1965)
156 Tornadoes	893 Tornadoes	47 Tornadoes

AREA — JAPAN: 6 (TR), 30 (DM), 42% (MI), 21 (ME), 1 (MA), (GI), (DG)

AREA — UNITED STATES: 21 (TR), 24 (DM), 29% (MI), 16 (ME), 9 (MA), 1 (GI), 0.1 (DG)

AREA — PALM SUNDAY: 4 (TR), (DM), 15 (MI), 15 (ME), 53% (MA), 11 (GI), 2 (DG)

INTENSITY — JAPAN: 40 (FO), 40 (FI), 17% (F2), 3 (F3), (F4), (F5), (F6)

INTENSITY — UNITED STATES: 33 (FO), 44% (FI), 17 (F2), 5 (F3), 1 (F4), 0.1 (F5), (F6)

INTENSITY — PALM SUNDAY: 4 (FO), 27% (FI), 26 (F2), 26 (F3), 17 (F4), (F5), (F6)

Fig. 8. Typical distribution of tornado frequencies as functions of both area and intensity.

due mainly to the improvement in reporting systems. It is very likely that Japanese-type distribution is applicable to mo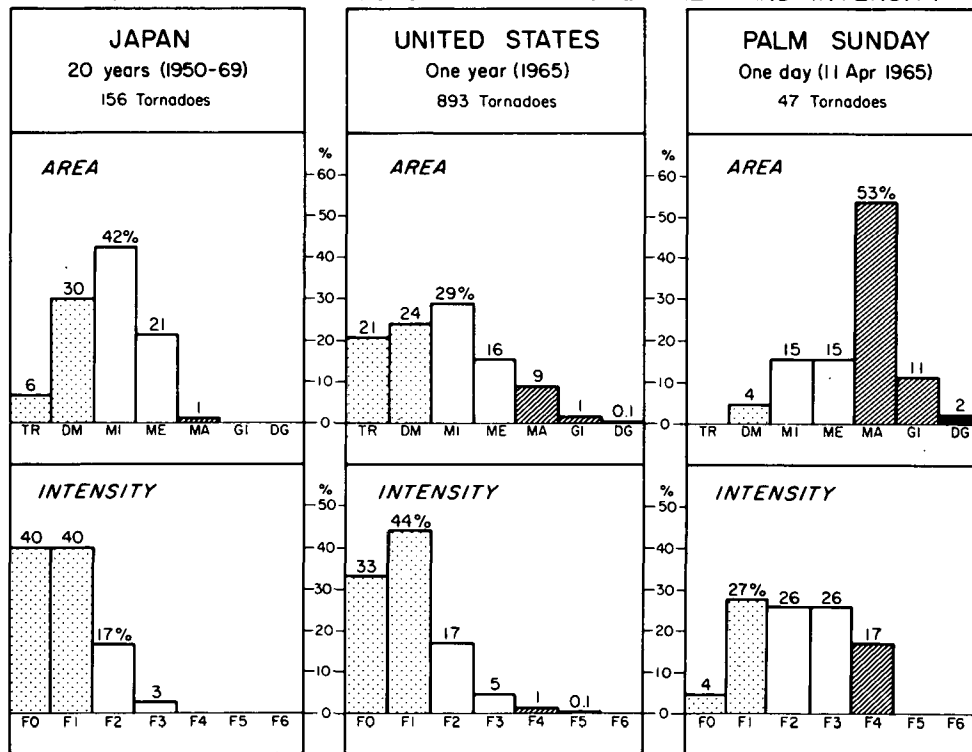st other island countries such as New Zealand, England, Italy, etc., where local weather bureaus have not been predicting tornadoes successfully. However, meteorological conditions giving rise to the formation of weak and/or small U.S. tornadoes could be found in other parts of the world if we look for them. For the improvement of U.S. local forecasts, investigation of unique conditions associated with large and strong tornadoes is of vital importance.

Further application of intensity and area characterization appears in Fig. 9. The figures on the left side show that autumn is the tornado season in Japan. It is seen that the intensity of tornadoes decreases in the spring as well as their monthly occurrences.
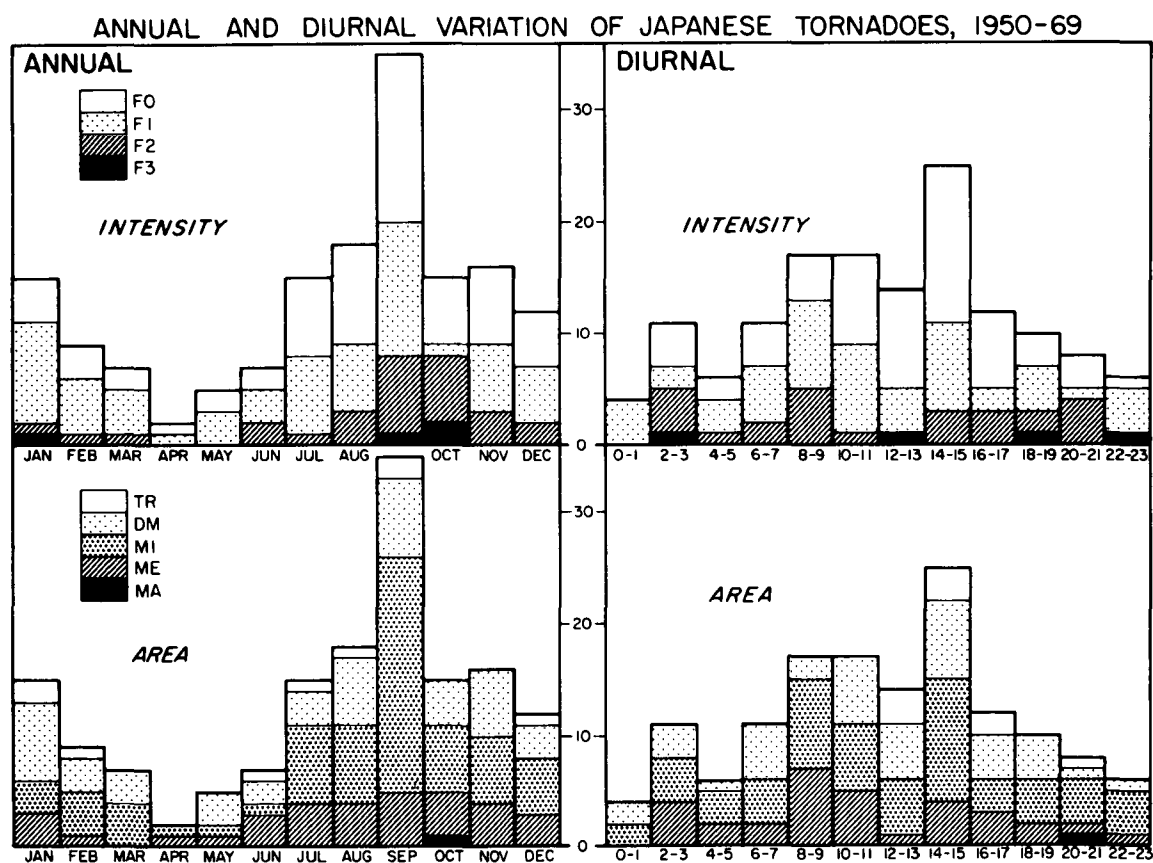

Fig. 9. Variation of characterized frequencies of Japanese tornadoes in 20-year period, 1950-1969. Unlike U.S. tornadoes, autumn is the tornado season with a significant minimum in April. Intense, F 2 and F 3 tornadoes are most frequent in September and October when large-area storms are also expected. Note that diurnal variation of Japanese tornadoes is insignificant.

21

Diurnal variation (right side) shows an overall maximum around local noon, but the strong ones, F 2 and F 3, remain active nearly 24 hours a day. It is of interest to find that the maximum frequency of Meso tornadoes, the largest category with the exception of one Macro tornado, occurred between 8 and 9 in the morning. The intensity also shows a maximum at this time. Meteorological reasons for these occurrences have not been explored.

8. APPLICATION OF F SCALE TO THE SURVEY OF HURRICANE DAMAGE

Unlike tornadic storms, hurricanes and typhoons are long lived, covering and affecting large areas. From meteorological points of view these storms have been characterized by their parameters which are measured by satellite, radar, vertical soundings, aircraft, and other means of observations. Moreover, most meteorological instruments are designed and constructed to withstand most hurricanes and typhoons.

Since measured winds are more accurate than estimated F-scale winds, it is not necessary to determine F-scale winds if nearby anemometers are available. In reality, however, the number of anemometers existing inside a vast area of storm damage is so inadequate that both ground and aerial surveys are required to determine meso to micro-scale damage patterns caused by typhoons and hurricanes. F-scale estimates inside hurricane areas are, therefore, very useful in establishing the patterns of damaging wind, which cannot be determined by using only a limited number of anemometers.

Presented in Fig. 10 is the distribution of F-scale winds inside hurricane Camille of August 17-18, 1969 when the storm travelled inland. F-scale winds and their directions were determined by the author from an aerial survey a few days after the storm. There were only several wind recorders within the damage area, making it very difficult to establish damage patterns based exclusively on measured wind speeds.

It should be noted that the RECON winds inside Camille prior to the landing were about F 4 equivalent, which was considerably stronger than F 3, the highest value of the F scale wind estimated near the storm's landing site. Such a difference could be related to the weakening of the storm, the nature of RECON and anemometer winds, etc.

It is worthwhile, at this point, to reexamine various definitions of wind speeds so as to inter-relate them as much as possible. Strictly speaking, however, there is no way of converting one type of wind into others because the time variation of wind speed cannot
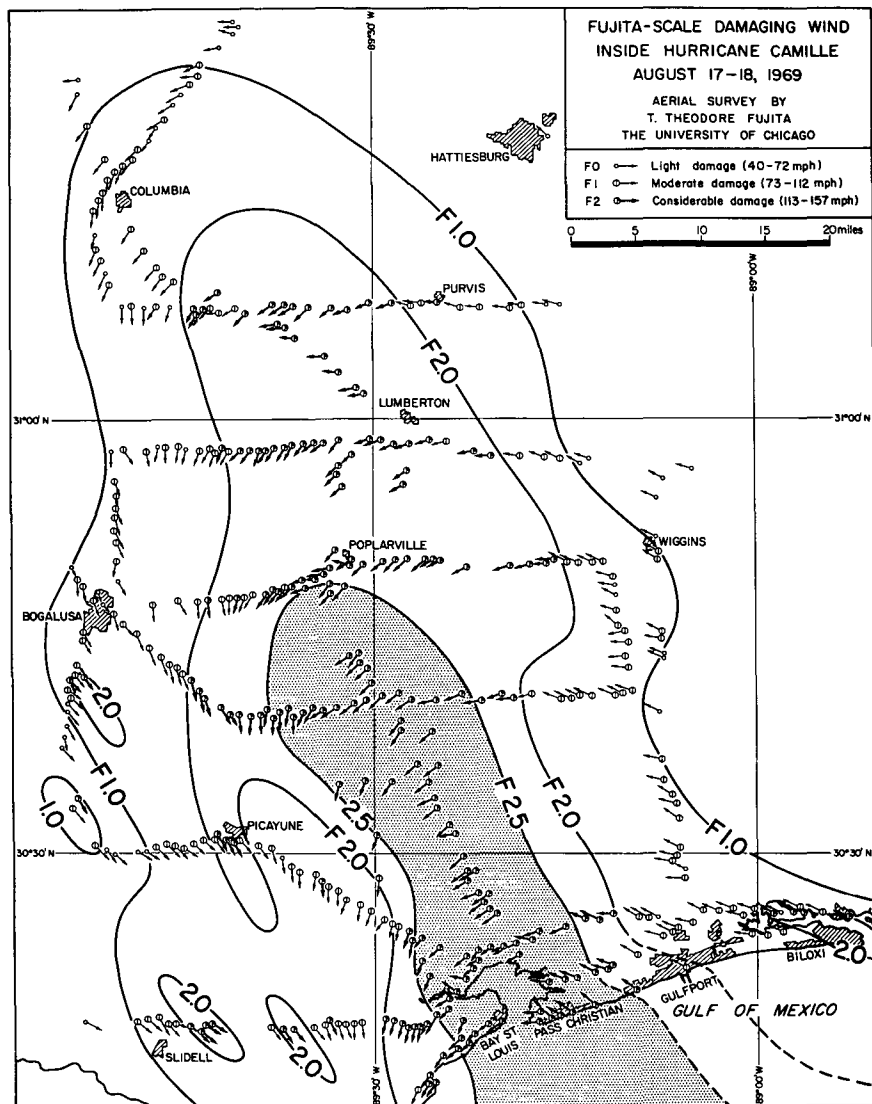
Fig. 10. Distribution of F-scale damage caused by hurricane Camille of August 17-18, 1969.

be expressed as a simple periodic function. The following terms are used in this paper to express the nature of the measured wind.

FASTEST 10-MIN WIND or Maximum 10-min Wind

The maximum wind speed averaged over any ten-minute period at a given station during a specified period.

FASTEST 1-MIN WIND or Maximum 1-min Wind

The maximum wind speed averaged over any one-minute period at a given station during a specified period.

PEAK GUST or Maximum Instantaneous Wind

The highest instantaneous wind speed at a given station within a specified period.

FASTEST MILE WIND

The maximum speed of any mile-passage of wind at a given station during a specific period. The averaging period decreases inversely proportional to the fastest mile wind speed.

FASTEST 1/4 MILE WIND or F-scale Damaging Wind

The maximum speed of any 1/4 mile-passage of wind at a given station during a specified period. The averaging period decreases inversely proportional to F-scale wind speed.

Because these five wind measurements are not always available simultaneously from each station affected by a specific storm, it is desirable to establish certain relationships between these winds, with the understanding that the relationships are approximate.

It is customary to express the peak gust as a function of both mean wind speed and gustiness factor, thus

$$V_{PG} = (1 + \frac{1}{2} g) \overline{V}_{10 \text{ or } 1} \tag{5}$$

where V_{PG} denotes the peak gust, g the gustiness factor defined by

$$g = \frac{\text{gust speed} - \text{lull speed}}{\text{mean wind speed}},$$

and $\overline{V}_{10}$ and $\overline{V}_{1}$, the 10-min and 1-min mean speed, respectively. The gustiness factors vary widely from storm to storm as well as the location of anemometers. As shown in a scatter diagram of Fig. 11, the gustiness factors of most typhoons in Japan are between 0.3 and 1.5, indicating that the range of lull to gust speeds is comparable to the mean speed.
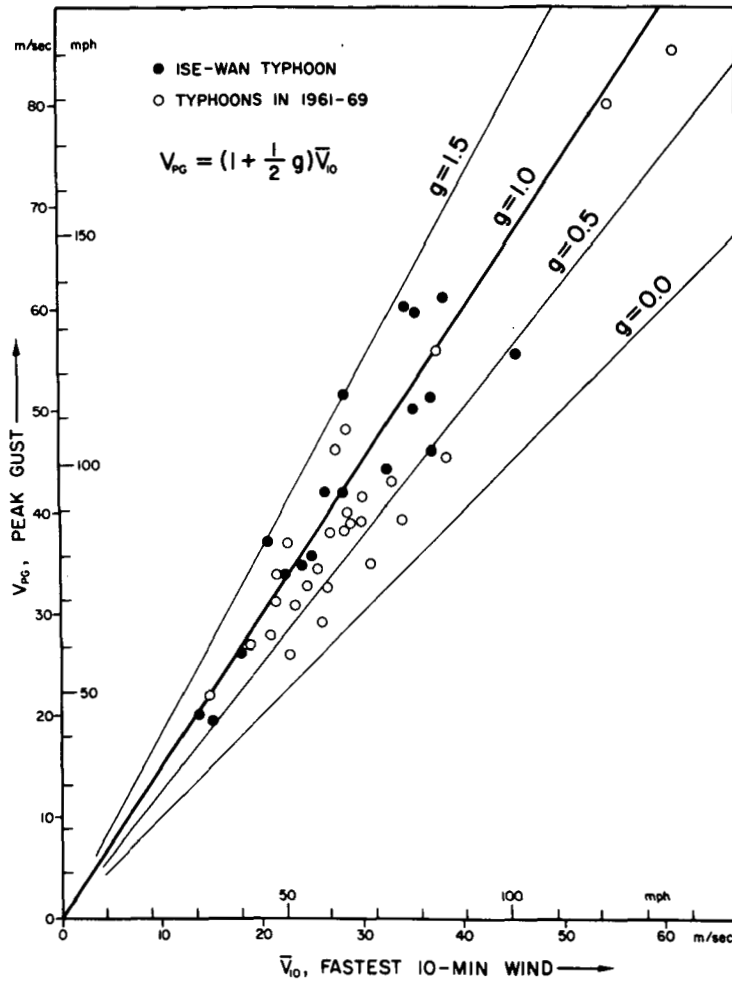
24

Fig. 11. Scatter diagram indicating a linear relationship between the peak gust and the fastest mean wind of Japanese typhoons. The gustiness factor, g , can be approximated as 1.0. Data points indicated by black dots represent the values measured within Ise-wan Typhoon of 26 September 1959. The number of dead and missing due to this hurricane was about 5000.

As a first approximation we express the wind speed by a sinusoidal gust superimposed upon the mean wind velocity $\overline{V}$, thus

$$V = f(t) = \overline{V} + \frac{1}{2} g \overline{V} \cos \frac{2\pi t}{p} \tag{6}$$

where p denotes the period of the sinusoidal gust (see Fig. 12). So long as the period p is much shorter than the averaging period, one or ten minutes, the averaging period does not alter the mean value. Eq. (5) can thus be written simply as

$$V_{PG} = (1 + \frac{1}{2} g) \overline{V} . \tag{7}$$

The fastest 1/4-mile or F-scale damaging wind can be obtained by integrating the wind passage centered at the time of the peak gust. Namely, we write
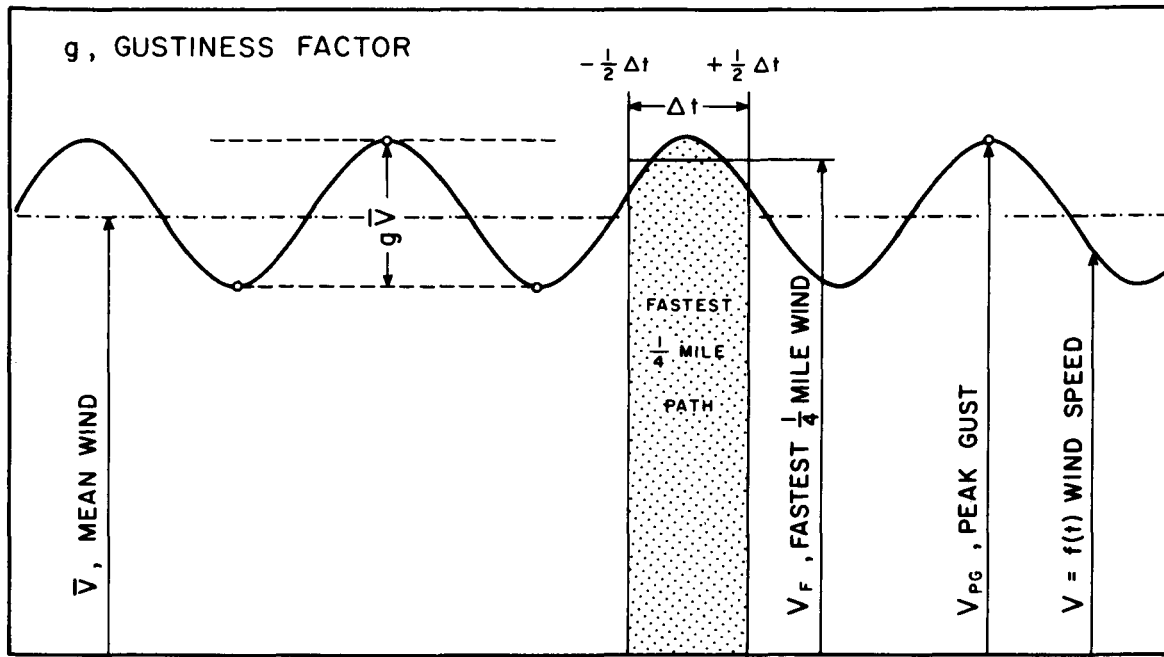
25

Fig. 12. Time variation of a simplified gusty wind. The wind speed as a function of time is expressed by a sinusoidal variation superimposed upon a constant wind.

$$V_F \, \Delta t = \frac{1}{4} \text{ mile} = \int V \, dt$$

$$= \overline{V} \Delta t + \frac{g p \overline{V}}{4 \pi} \left[\sin \frac{2 \pi t}{p} \right]_{-\frac{1}{2}\Delta t}^{+\frac{1}{2}\Delta t}$$

$$= \overline{V} \Delta t + \frac{g p \overline{V}}{2 \pi} \sin \frac{\pi \Delta t}{p} \tag{8}$$

where Δt is the time in which the F-scale wind travels through a distance of 1/4 mile at the rate of V_F, the speed of the fastest 1/4 mile wind.

Substituting Δt in Eq. (8) by $\frac{1}{4V_F}$, we have

$$\frac{1}{4} \text{ mile} = \frac{\overline{V}}{4V_F} + \frac{g p \overline{V}}{2 \pi} \sin \frac{\pi}{4 p V_F}$$

or
$$\overline{V} = \left(\frac{1}{V_F} + \frac{2 g p}{\pi} \sin \frac{\pi}{4 p V_F} \right)^{-1} \tag{9}$$

From this equation, we are able to convert F-scale wind speed, V_F, into the mean wind speed, $\overline{V}$. It should be noted, however, that both gustiness factor, g, and period, p, must be known for the conversion.

In special cases when V_F is extremely high or low, Eq. (9) can be reduced

26

simply to

$$V_F = \overline{V} \qquad\qquad \text{for very low wind speeds} \qquad\qquad (10)$$

and

$$V_F = \overline{V} \left(1 + \tfrac{1}{2} g\right) \quad \text{for very high wind speeds} \qquad\qquad (11)$$

because the sinusoidal term in Eq. (9) becomes small in comparison with the other term and may be neglected when V_F is small and the sinusoidal term can be approximated as $\tfrac{1}{2} g / V_F$ for large values of V_F.

The above approximation implies that the damage caused by an extremely high wind is closely related to the peak-gust speed as expressed by Eqs. (7) and (11). On the other hand, weak damage due to low winds, such as 40 mph, is a result of the time integrated stress of repeated weak gusts and a steady flow of air against weak structures.

Two gustiness parameters, g and p, are closely related to the turbulent characteristics of damaging winds which are usually highly gusty near the ground. For hurricanes and typhoons the gust period varies between the order of seconds and minutes. For tornadoes, however, little is known regarding their gustiness characteristics. A tornado wind trace recorded by the Tecumseh Health Study, University of Michigan and reported by Fujita et al. (1970) in their Palm Sunday Tornado paper, showed a 151 mph peak gust characterized by a gust period of about 20 seconds.

Coming back to the problem of converting F-scale wind speeds into anemometer-measured wind speeds, it should be emphasized that the mean wind speed represents F-scale wind speed when the speed is very low and that F-scale speed approaches the peak gust speed as the speed increases. Figure 13 shows two dotted straight lines representing the mean and peak gust speeds. In computing the mean speed as a function of F-scale speed using Eq. (9), two gustiness periods, 15 sec and 30 sec, were assumed. These curves in Fig. 13 shown in short and long dashed lines respectively, reveal, as expected, that the F-scale wind is very close to the peak gust when the speed is in excess of 150 mph. This is because the maximum damage occurs mostly at the time of the peak gust. As the wind speed decreases, both dashed lines approach the mean speed line in damped oscillatory manners because Eq. (9) includes a sinusoidal term. By specifying a number of gustiness periods, the same number of dashed lines are to be added in the figure.
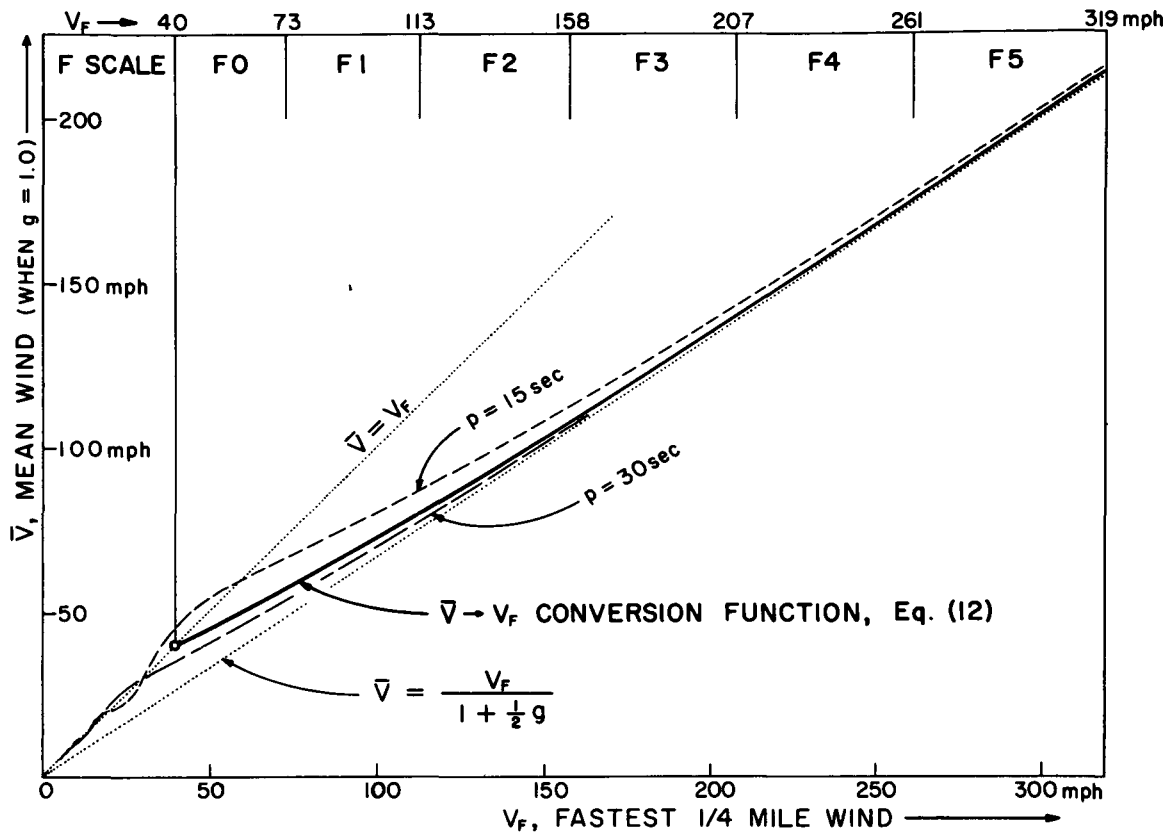
Fig. 13. A function to convert fastest 1/4 mile wind into mean wind and peak gust.

Since it is impractical to produce conversion functions corresponding to a number of gustiness periods, a specific gustiness period was selected for the conversion purposes. The period was selected so that the conversion curve connects smoothly the 40 mph or F0 wind speed with the peak gust speed. A heavy line departing from $\bar{V}$ = V_F = 40 mph represents the proposed conversion function (see Fig. 13). The gustiness period for this conversion function can be obtained by selecting the angles to reduce the sinusoidal term in Eq. (9) to zero. These angles are 0, π , 2π, ... $n\pi$. In view of the fact that 0 represents V_F = infinity, the next larger angle, π should be used for this purpose. Thus we equate π with the angle in Eq. (9), thus

$$\pi = \frac{\pi}{4pV_F} \quad \text{or} \quad p = \frac{1}{4V_F}$$

28

in mph units. Putting V_F = 40 mph as originally assumed, we have

$$p = \frac{1}{4 \times 40} \text{ hour} = \frac{3600}{160} \text{ sec} = 22.5 \text{ sec} .$$

The equations for converting V_F into $\overline{V}$ and V_{PG} are thus expressed in mph by

$$\overline{V} = \frac{1}{\dfrac{1}{V_F} + \dfrac{45g}{\pi} \sin \dfrac{\pi}{90 \, V_F}} \qquad (12)$$

and

$$V_{PG} = \frac{1 + \frac{1}{2}g}{\dfrac{1}{V_F} + \dfrac{45g}{\pi} \sin \dfrac{\pi}{90 \, V_F}} \qquad (13)$$

These equations can readily be used in relating F-scale wind speed, V_F , with both fastest mean speeds and peak gust speeds measured and/or recorded by anemometers. It should be emphasized that the period of the fastest mean speed, averaged over one- or ten-minutes, must be selected as being close to the time of the occurrence of the fastest 1/4 mile wind. Such a selection will permit us to approximate actual winds as a simple sinusoidal function expressed by Eq. (6) and Fig. 12.

9. USE OF TABLE CONVERTING MEASURED WINDS INTO F SCALE WINDS FOR HURRICANES

Unlike wind records within a tornado, a large number of measured maximum winds is available within a specific hurricane during its life time. These winds are reported in forms of FASTEST 10- or 1-MIN WIND, PEAK GUST, FASTEST MILE WIND, RECON WIND, and others.

In order to relate these winds with detailed patterns of F-scale winds, which can be mapped with isolines of F0, F1, F2, etc., it is necessary to convert these measured winds into F-scale wind. Although the F scale estimates from structural and/or tree damage are just enough to distinguish the stepped F-scale values, measured wind speeds are to be converted into the fractional scales such as F0.3, F2.3, F3.0 etc., thus allowing the determination of more accurate values at anemometer locations but not everywhere over the areas of wind damage caused by a storm.

Table IV, computed from Eqs. (12) and (13), permits us to determine fractional F-scale values from measured wind speeds at 2 m/s intervals given in three units, m/s,

29

Table IV. TABLE TO ESTIMATE FUJITA SCALE FROM RECON WIND, PEAK GUST, AND MEAN WIND. Gustiness factor, g, may be assumed 1.0 for most land stations. g = 1.5 can be applied to very gusty winds often observed at inland stations and g = 0.5 to light gust conditions. To determine F scale, first estimate gustiness factor at the top, then look down the appropriate column to the measured wind speed given in m/s, kt, and mph.

MEASURED WIND SPEED			RECON WIND		PEAK GUST			MEAN WIND		
m/s	kt	mph	g=0.0	g=0.1	g=0.5	g=1.0	g=1.5	g=0.5	g=1.0	g=1.5
18	35	40	F 0.0	F 0.0	–	–	–	F 0.0	F 0.0	F 0.0
20	39	45	F 0.1	F 0.1	–	–	–	F 0.2	F 0.3	F 0.4
22	43	49	F 0.3	F 0.3	–	–	–	F 0.4	F 0.6	F 0.8
24	47	54	F 0.4	F 0.4	F 0.0	–	–	F 0.6	F 0.8	F 1.1
26	51	58	F 0.6	F 0.6	F 0.2	–	–	F 0.8	F 1.0	F 1.4
28	54	63	F 0.7	F 0.7	F 0.4	F 0.0	–	F 0.9	F 1.2	F 1.6
30	58	67	F 0.8	F 0.8	F 0.6	F 0.3	–	F 1.1	F 1.4	F 1.8
32	62	72	F 1.0	F 1.0	F 0.7	F 0.5	F 0.0	F 1.2	F 1.6	F 2.0
34	66	76	F 1.1	F 1.1	F 0.8	F 0.6	F 0.3	F 1.4	F 1.8	F 2.2
36	70	81	F 1.2	F 1.2	F 1.0	F 0.8	F 0.6	F 1.6	F 2.0	F 2.4
38	74	85	F 1.3	F 1.3	F 1.1	F 0.9	F 0.8	F 1.7	F 2.1	F 2.6
40	78	90	F 1.4	F 1.5	F 1.2	F 1.1	F 1.0	F 1.9	F 2.3	F 2.8
42	82	94	F 1.5	F 1.6	F 1.3	F 1.2	F 1.1	F 2.0	F 2.5	F 3.0
44	86	98	F 1.7	F 1.7	F 1.5	F 1.4	F 1.3	F 2.1	F 2.6	F 3.1
46	89	103	F 1.8	F 1.8	F 1.6	F 1.5	F 1.4	F 2.2	F 2.8	F 3.3
48	93	107	F 1.9	F 1.9	F 1.7	F 1.6	F 1.5	F 2.4	F 2.9	F 3.4
50	97	112	F 2.0	F 2.0	F 1.8	F 1.7	F 1.7	F 2.5	F 3.1	F 3.6
52	101	116	F 2.1	F 2.1	F 1.9	F 1.8	F 1.8	F 2.6	F 3.2	F 3.8
54	105	121	F 2.2	F 2.2	F 2.0	F 1.9	F 1.9	F 2.7	F 3.3	F 3.9
56	109	125	F 2.3	F 2.4	F 2.1	F 2.1	F 2.0	F 2.9	F 3.5	F 4.1
58	113	130	F 2.4	F 2.5	F 2.3	F 2.2	F 2.1	F 3.0	F 3.6	F 4.2
60	117	134	F 2.5	F 2.6	F 2.4	F 2.3	F 2.2	F 3.1	F 3.8	
62	120	139	F 2.6	F 2.7	F 2.5	F 2.4	F 2.3	F 3.2	F 3.9	
64	124	143	F 2.7	F 2.8	F 2.6	F 2.5	F 2.4	F 3.3	F 4.0	
66	128	148	F 2.8	F 2.9	F 2.7	F 2.6	F 2.5	F 3.4	F 4.1	
68	132	152	F 2.9	F 3.0	F 2.8	F 2.7	F 2.7	F 3.6	F 4.2	
70	136	157	F 3.0	F 3.1	F 2.9	F 2.8	F 2.8	F 3.7		
72	140	161	F 3.0	F 3.2	F 3.0	F 2.9	F 2.9	F 3.8		
74	144	166	F 3.1	F 3.3	F 3.1	F 3.0	F 3.0	F 3.9		
76	148	170	F 3.2	F 3.4	F 3.2	F 3.1	F 3.1	F 4.0		
78	152	175	F 3.3	F 3.5	F 3.2	F 3.2	F 3.2	F 4.1		
80	155	179	F 3.4	F 3.6	F 3.3	F 3.3	F 3.3	F 4.2		
82	159	183	F 3.5	F 3.7	F 3.4	F 3.4	F 3.4			
84	163	188	F 3.6	F 3.8	F 3.5	F 3.5	F 3.4			
86	167	192	F 3.7	F 3.8	F 3.6	F 3.6	F 3.5			
88	171	197	F 3.8	F 3.9	F 3.7	F 3.7	F 3.6			
90	175	201	F 3.9	F 4.0	F 3.8	F 3.7	F 3.7			
92	179	206	F 4.0	F 4.1	F 3.9	F 3.8	F 3.8			
94	183	210	F 4.0	F 4.2	F 4.0	F 3.9	F 3.9			
96	187	215	F 4.1	F 4.3	F 4.1	F 4.0	F 4.0			
98	190	219	F 4.2	F 4.4	F 4.1	F 4.1	F 4.1			

kt, and mps. Three types of winds, RECON, PEAK GUST, and MEAN WINDS, are tabulated because they are usually reported to express hurricane winds. To determine the F scale, first estimate the gustiness factor given at the top, then follow the appropriate column down to the measured wind speed given in the left three columns.

RECON winds are one of the most important parameters to estimate the intensity of hurricanes over the ocean. An example of Doppler winds measured at 1770 ft through the eye of hurricane Gladys of 17 October 1968 is shown in Fig. 14. Most data points,
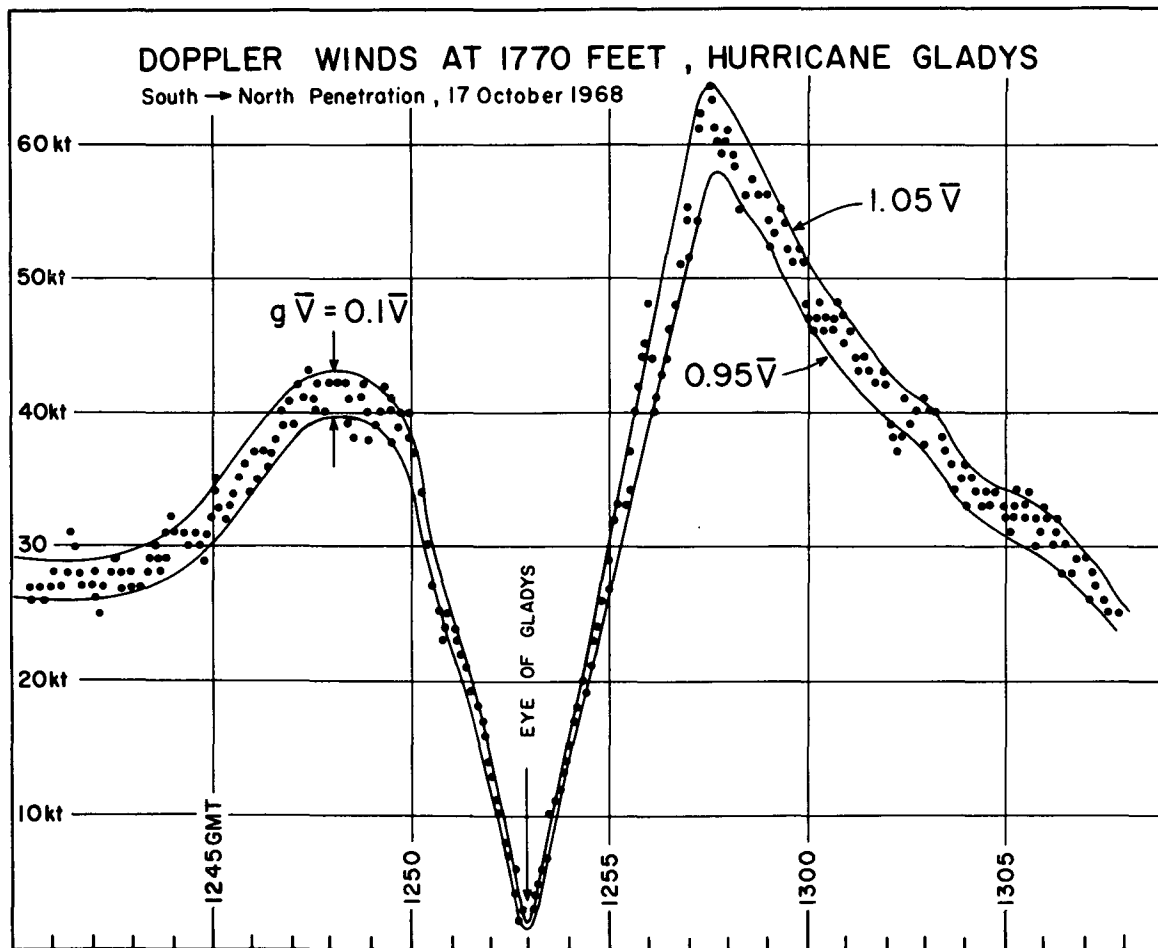
Fig. 14. Doppler winds measured at 1770 ft through the eye of hurricane Gladys on October 17, 1968. Winds were measured by RFF's DC6B while traversing south to north during the research mission.

plotted for every 5-sec, are within 0.95 and 1.05 of the center values about which the wind fluctuates. F-scale winds in g = 0.1 column were computed from Eq. (12) assuming that RECON wind represents the center value. If the gustiness factor is zero, the left

31

column for g = 0.0 should be used for conversion of such RECON winds into F-scale values. It is likely that gustiness factor for RECON winds is much smaller than that of turbulent wind recorded at the levels of structures on the ground.

Both PEAK GUST and MEAN winds are tabulated for three gustiness factors, 0.5, 1.0, and 1.5. For most wind stations g = 1.0 may be used for practical purposes. For very gusty wind, g = 1.5 will result in a better approximation. With this gustiness factor, the lull to gust speed will vary from 0.25 to 1.75 times the mean wind speed. For insignificant gust cases which are likely to occur at coastal stations or land stations at night, the use of g = 0.5 is often appropriate.

Some stations report both PEAK GUST and the corresponding MEAN WIND. Each of these values can be used to determine the F scale independently by assuming a gustiness factor. Two F scales thus estimated independently could differ significantly because the gustiness factor assumed may not be accurate enough. If they differ beyond an allowable limit of 0.2 to 0.3 in F scale, we may use the mean values of the two estimated F scales. For example, if reported hurricane winds from a station are 130 mph PEAK GUST and 90 mph MEAN WIND, Table IV gives F scales corresponding to these values as being

F 2.3   and   F 1.9   for   g = 0.5
F 2.2   and   F 2.3   for   g = 1.0
F 2.1   and   F 2.8   for   g = 1.5 ,

respectively, indicating that g = 1.0 turns out to be the best approximation because F 2.2 and F 2.3, estimated respectively from the peak gust and the mean wind, show very good agreement. If we compute the average F scales obtained by assuming g = 0.5 and g = 1.5 they are F 2.1 and F 2.4, respectively and each of these averages are close enough to F 2.2 and F 2.3 which would represent the appropriate F scale at this station. Nevertheless, the most reasonable estimate of F scale from Table IV can be performed by selecting a gustiness factor, g, which would minimize the difference in the F scales estimated independently from both peak gust and maximum mean speed occurring at a station during a specific hurricane.

Another example of F scale estimate from an anemometer record is shown based on a gust-recorder trace from Reynolds Metal Company located just north of the track of hurricane Celia of 1970. As shown in Fig. 15 the peak gust and the maximum mean wind were 138 mph and 110 mph ahead of the eye and 134 mph and 100 mph to the rear of the
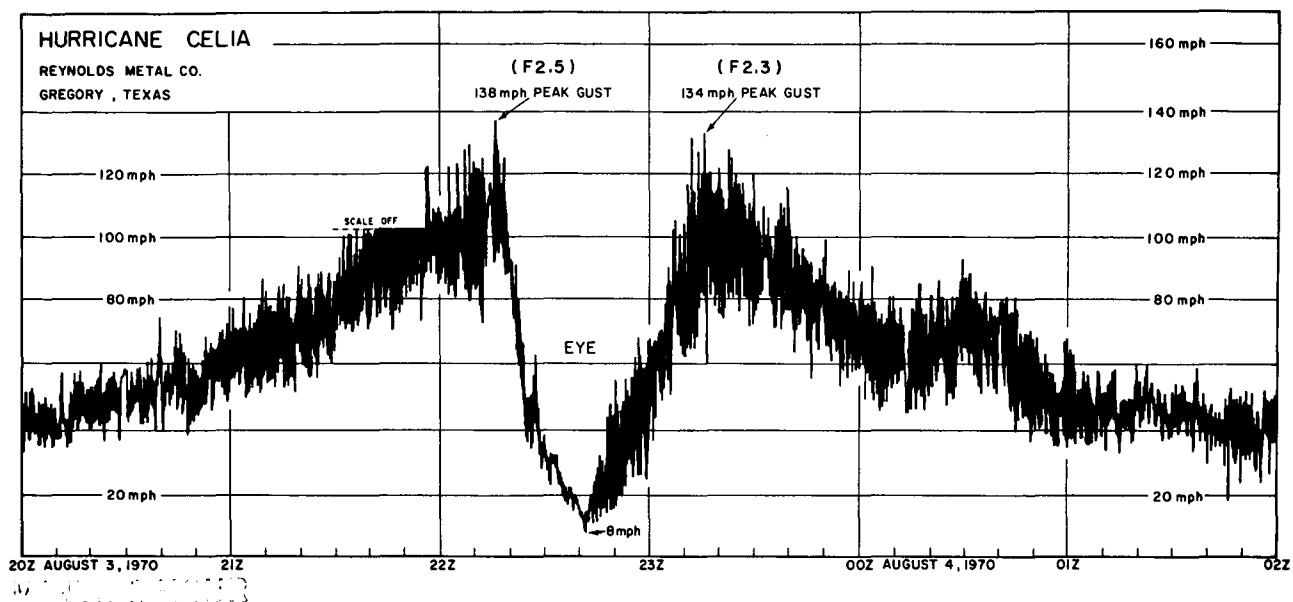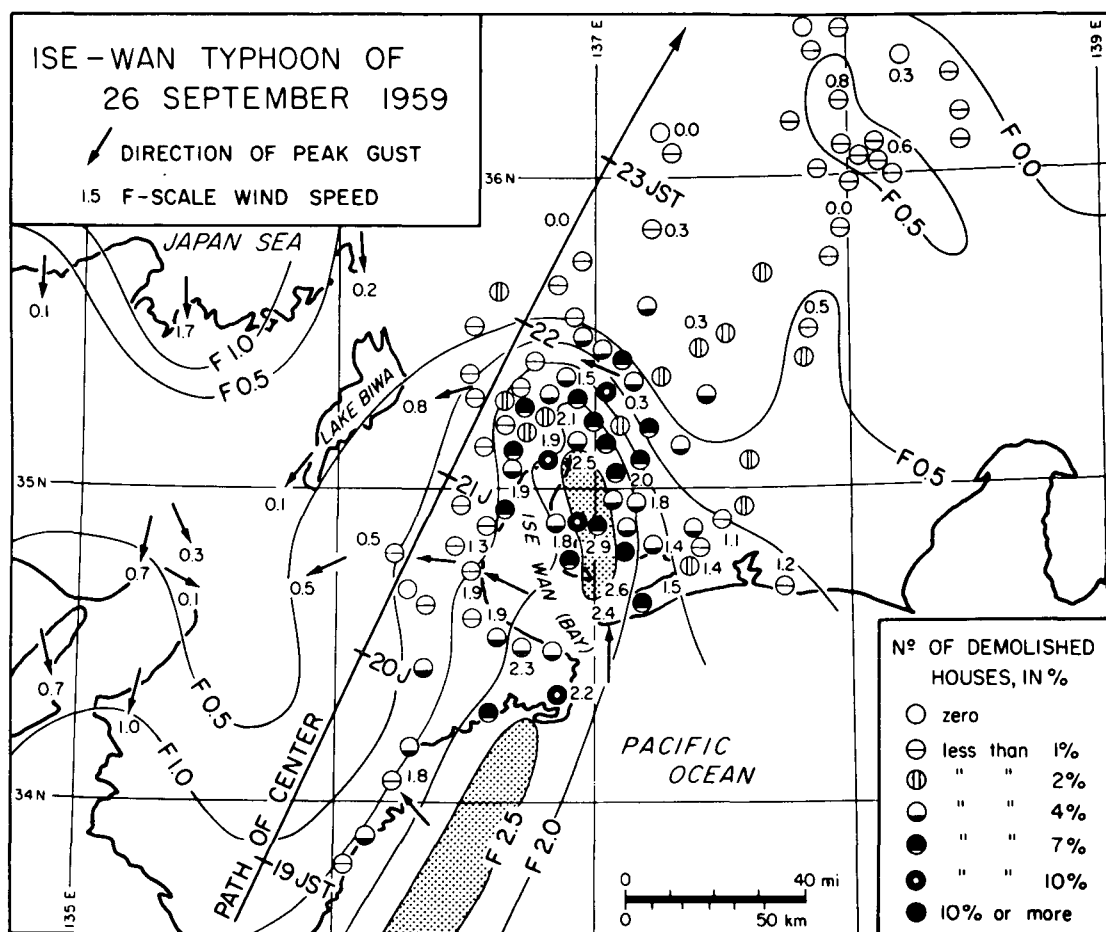
Fig. 15. Wind speed trace of Hurricane Celia, August 3-4, 1970 recorded at Reynolds Metal Company.

eye. These values result in the best possible F scale when g = 0.5 is applied. F scales for this storm before and after the passage of the eye are thus estimated to be F2.5 and F 2.3, respectively.

Reynolds Metal Company was located to the right of Celia's center, where the strongest hurricane winds are expected. Simpson's (1970) aerial survey and subsequent investigation revealed that the storm damage occurring predominantly on the left side of the track was caused by strong westerly winds. The westerly winds were estimated to be stronger than those on the other side, causing considerable damage in Corpus Christi. Since dynamical aspects of the hurricane circulation resulting in such damage are quite unusual, a joint research between Dr. Simpson and the author was initiated and fine patterns of damage streaks are being obtained.

In order to demonstrate structural damage in relation to the pattern of F-scale wind, distribution of damaged houses reported by Ishizaki et al. (1961) was combined with F-scale winds. As shown in Fig. 16, the Ise-wan typhoon packed with 150 mph winds in the eastern sector of the 930 mb center landed near the southern tip of Kii peninsula shortly before 1900 Japan Standard Time. During the next 3 hours a tongue of up to F 2.9 winds moved north, resulting in a 3.6-m or 12-ft storm surge and 5,000 fatalities. In

33

Fig. 16. Relation between the F-scale wind and the relative number of houses demolished by the Ise-wan Typhoon of 26 September 1959 which diagonally crossed the central part of Japan.

Nagoya City 6,569 houses out of 252,145 were demolished due mostly to strong wind. Further examination of Fig. 16 together with the original data and analyses by the above authors revealed that 10% of Japanese houses will be demolished by a F 3.0 wind, 5% by F 2.0 wind. No demolished houses are reported in areas where the fastest wind was less than F 0.0.

Although the F-scale analysis of the Ise-wan typhoon cannot be pursued further, meso- to microscale patterns of F-scale winds can be determined if local aerial photographs covering the storm-stricken area were available.

10. CHARACTERIZATION OF HURRICANES AND TYPHOONS

For the purpose of determining the statistical differences in the maximum wind speeds of Pacific typhoons, Atlantic hurricanes, and Pacific hurricanes, maximum wind speeds of all storms tabulated in the National Summary, Climatological Data (1960-69) were chosen to obtain cumulative numbers of storms as a function of F scale converted from the published maximum speeds which are based on various types of measurements. The result summarized in Fig. 17 shows that 34 Pacific hurricanes leveled off before
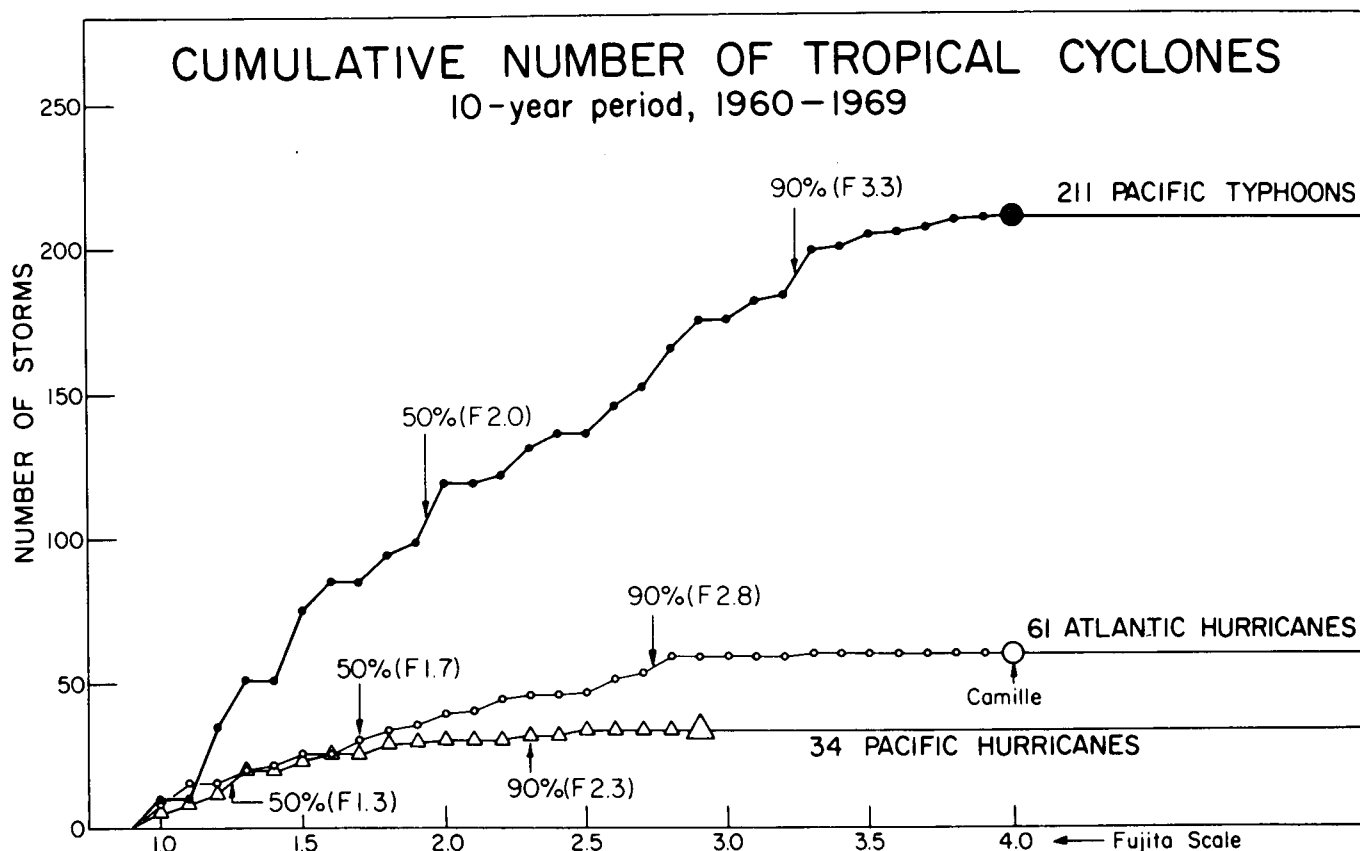
Fig. 17. Cumulative number of tropical cyclones during a 10-year period, 1960-1969, plotted against Fujita scale wind speed.

reaching F 3.0, while Atlantic hurricanes, 61 in total number, kept increasing their cumulative number until Camille of 1969 hit F 4.0.

Pacific typhoons occurred almost 3.5 times more often than hurricanes but the maximum F scale was very close to that of Camille. The F scale corresponding to the

35

90% cumulative numbers vary among these species of storms. Namely, 90% of Pacific hurricanes are less than F 2.3, Atlantic hurricanes, less than F 2.8, but 90% of Pacific typhoons may be up to F 3.3.

In an attempt to determine the relationship between the central pressure and F-scale wind speed, a scatter diagram (see Fig. 18) was made by plotting the central
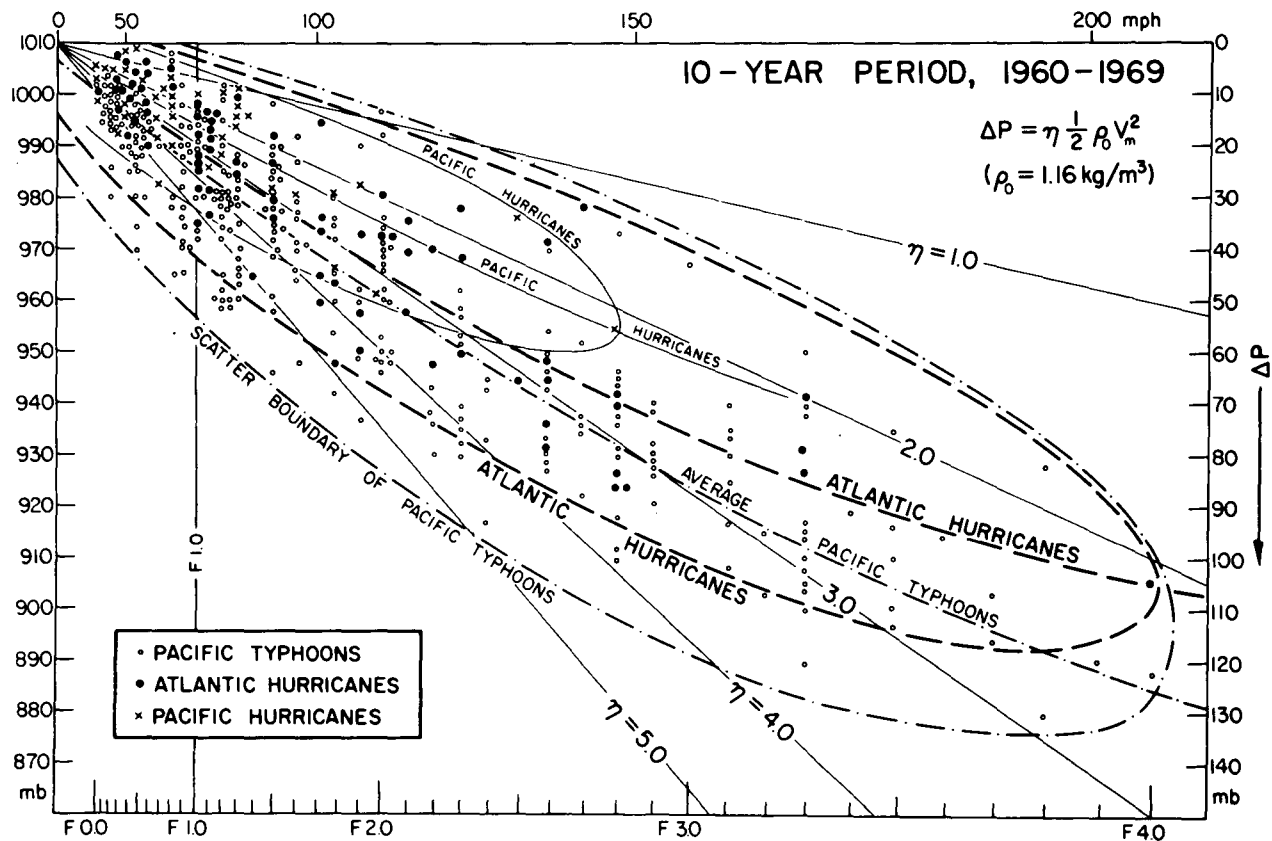
Fig. 18. A scatter diagram showing the central pressures of hurricanes and typhoons plotted against F-scale wind speed. Note that three species of storms, each enclosed by an elongated ellipse, are slightly different. For a given wind speed, central pressures of Pacific typhoons in average are lower than hurricanes.

pressures of 1960-69 storms against

$$V^2 = 39.7 (F + 2)^3 \ m^2/sec^2 = 199 (F + 2)^3 \ mph^2 \tag{14}$$

which is obtained as the square of Eq. (2).

If hurricanes and typhoons are assumed to be Rankine-type vortices with cyclostrophically balanced wind everywhere, the pressure deficit at the center is given by

36

$$\Delta P = 2 \cdot \frac{1}{2} \rho V_m^2 \qquad\qquad (15)$$

where ρ is the density of air assumed to be constant and V_m , the speed of the maximum wind around the eye wall.

Figure 18 reveals, however, that the "pressure-deficit coefficient", η defined by

$$\Delta P = \eta \frac{1}{2} \rho_0 V_m^2$$

where ρ_0 = 1.16 kg/m³ at 1010 mb and 30°C virtual temperature or about 27°C air temperature, varies widely between 1 and 5 or more. A slight variation of ρ , which was neglected in obtaining Eq. (15), does not produce such a variation. Moreover, the average scatter for each storm group shows a successive shift from Pacific typhoons to Atlantic hurricanes to Pacific hurricanes. This means that F-scale maximum wind speed as well as the radial distribution of tangential wind speed are needed for an improved characterization of tropical cyclones.

If we approximate tangential wind speeds inside and outside the circle of the maximum wind, respectively, by

$$V = k_a r^a \quad \text{where} \quad k_a = V_m / r_m^a \qquad \text{(inside)}$$

and

$$V = k_b r^{-b} \quad \text{where} \quad k_b = r_m^b V_m \qquad \text{(outside)} , \qquad (16)$$

cyclostrophic approximation will permit us to write

$$\eta = \eta_a + \eta_b \qquad\qquad (17)$$

where $\eta_a = \dfrac{1}{a}$ and $\eta_b = \dfrac{1}{b}$

and a is estimated to be larger than 1 and b is smaller than 1 and close to 0.5 according to Riehl (1954). By selecting proper values of a and b , we will be able to characterize both Pacific and Atlantic storms in terms of intensity and radial distribution of wind.

These evidences imply that the central pressure of hurricanes and typhoons cannot be related to the maximum F-scale wind speed without accepting a large standard deviation. For a given F-scale wind, the central pressure seems to vary as much as 50 mb throughout the range of hurricane F-scale winds. If such variations are caused by the deviation of hurricane and typhoon vortices from simplified Rankine vortices, proper interpretation of η , taking into consideration the dynamical aspects of the circulation as well as Coriolis force, will be of vital importance.

Nonetheless, the scatter diagram of Fig. 18 clearly shows major statistical differences between Atlantic hurricanes, Pacific hurricanes, and Pacific typhoons which are to be characterized by various parameters.

11. CONCLUSIONS

Numerous severe storms such as hailstorms, tornadoes, tropical cyclones, etc. are spawning and dying out after minutes or days of their life given by Mother Nature. Unlike human beings or others in the animal world, individual storms belonging to one species are so different in size and intensity that each must be characterized properly in order to assess their behavior and effects on human life.

Investigations of U.S. and Japanese Storm Data revealed that the area affected by an individual storm reported as a tornado or tatsumaki is less than 0.001 sq. mi., while the largest one in U.S. was in excess of 100 sq. mi., or 1:1,000,000 in areal ratio. The range of the maximum wind speed inside storms reported in Storm Data as tornadoes varies between less than 73 mph, Beaufort 12 and up to about 300 mph. It is misleading to assess tornado activities relying heavily on their occurrences without describing individual characteristics.

In order to avoid the existing possibility that a tornado affecting 0.001 sq. mi. and the other affecting a 10 sq. mi. area are treated with equal weight in statistical analyses, the author proposed to categorize individual tornado area according to its logarithm. The maximum wind speeds inside tornadoes are also categorized by F-scale which was devised to connect the upper end of Beaufort force with the low end of Mach number.

Several test analyses of tornado area and intensity thus defined now appear to be very useful. A comparison of Japanese and U.S. tornadoes revealed that 75% of all tornadoes are similar in area and intensity distributions. The only difference is that U.S. has extremely large and/or strong tornadoes which do not exist in Japan. A further investigation of tornadoes in other parts of the world will probably result in similar distributions.

An initial attempt to investigate hurricane and typhoon damage with F-scale categories was made. The fact that the maximum F-scale damage expected in hurricanes and typhoons reaches F 3 permits the identification of damage into a maximum of three categories. This turned out to be very useful in estimating the fine structure of storm

circulation which cannot be studied otherwise.

Although this has been the first attempt to establish and identify storm character-istics by numbers obtained through an "educated guess", preliminary application presented in this paper revealed the potential value of the concept of "characterization".

REFERENCES

Battan, L. J. (1959): Duration of Tornadoes. Bull. Amer. Met. Soc., 40, 340-342.

Beebe, R. C. (1960): The Life Cycle of the Dallas Tornado. Research Paper No. 41, U. S. Weather Bureau, 3-52.

Brown, R. A. and T. T. Fujita (1961): Report on the Chicago Tornado of March 4, 1961, 13 pp.

Clarke, R. H. (1962): Severe Local Wind Storms in Australia. Div. of Meteor. Physics Tech. Paper No. 13, Commonwealth Scientific and Industrial Research Organization, Melbourne, Australia, 56 pp.

Climatological Data 1960-69: National Summary. U.S. Weather Bureau, NWRC, Asheville, N.C.

Court, A. (1970): Tornado Incidence Maps. ESSA Tech. Memorandum ERLTM-NSSL 49, NSSL, Norman, Okla., 76 pp.

Darkow, G. L. and J. C. Roos (1970): Multiple Tornado Producing Thunderstorms and their Apparent Cyclic Variations in Intensity. Preprints of 14th Radar Meteorology Conference, Tucson, Arizona, 305-308.

Flora, S. D. (1953): Tornadoes of the United States. University of Oklahoma Press, Norman, Oklahoma, 221 pp.

Fujita, T. T. (1960): A Detail Analysis of the Fargo Tornadoes of June 20, 1957. Research Paper No. 42, U. S. Weather Bureau, 67 pp.

Fujita, T. T. (1963): Analytical Mesometeorology: A Review. Meteorological Monograph 5, No. 27, 77-125.

Fujita, T. T. (1970): Estimate of Areal Probability of Tornadoes from Inflationary Reporting of their Frequencies. SMRP Research Paper No. 89, University of Chicago, 23 pp.

Fujita, T. T., D. L. Bradbury and C. F. Van Thullenar (1970): Palm Sunday Tornadoes of April 11, 1965. Monthly Weather Revue, 98, 29-69.

Hoecker, W. H., Jr. (1960a): The Dimensional and Rotational Characteristics of the Tornadoes and their Cloud System. Research Paper No. 41, U. S. Weather Bureau, 53-113.

Hoecker, W. H., Jr., (1960b): Wind Speed and Air Flow Patterns in the Dallas Tornado of April 2, 1957. Monthly Weather Revue, 88, 167-180.

Ishizaki, H., et al. (1961): Distribution of Structural Wind Damage Caused by the Ise-wan Typhoon (in Japanese). Annual Report No. 4, Disaster Prevention Research Institute, Kyoto University, Kyoto, Japan, 95-104.

Japanese Storm Data 1950-59: Kishoyoran (in Japanese). Japan Meteorological Agency, Tokyo, Japan.

List, R. J. (1958): Beaufort Wind Scale, Table 36, Smithsonian Meteorological Tables. Smithsonian Institution, Washington, D. C.

Melaragno, M. G. (1968): Tornado Forces and their Effects on Buildings. Kansas State University, 51 pp.

Pautz, E. M. (1969): Severe Local Storm Occurrences, 1955-1967. ESSA Tech. Memorandum WBTM FSST 12, Office of Meteorological Operation, Silver Springs, Maryland.

Penn, S., et al. (1955): The Squall Line and Massachusetts Tornadoes of June 9, 1953. Bull. Amer. Meteor. Soc., 36, 109-122.

Riehl, H. (1954): Tropical Meteorology. McGraw-Hill Book Co. Inc., New York, 392 pp

Segner, E. P., Jr., (1960): Estimates of Minimum Wind Forces Causing Structural Damage. Research Paper No. 41, U. S. Weather Bureau, 169-175.

Simpson, R. H. (1970): Personal Communication on Celia Damage.

Staats, W. F. and C. M. Turrentine (1956): Some Observations and Radar Pictures of Blackwell and Udall Tornadoes of May 25, 1955. Bull. Amer. Meteor. Soc., 37, 495-505.

Tecson, Jaime J. (1971): Characterization of 1965 Tornadoes by their Area and Intensity. SMRP Research Paper No. 94, University of Chicago.

Thom, H. C. S. (1963): Tornado Probabilities. Mon. Wea. Rev., 91, 730-736.

Van Tassel, E. L. (1955): The North Platte Valley Tornado Outbreak of June 27, 1955. Mon. Wea. Rev., 83, 239-254.

Wolford, V. L. (1960): Tornado Occurrences in the United States. Tech. Paper No. 20, U. S. Weather Bureau, Washington, D. C., 71 pp.

SUBJECT INDEX

MESOMETEOROLOGY PROJECT --- RESEARCH PAPERS

1.*   Report on the Chicago Tornado of March 4, 1961 - Rodger A. Brown and Tetsuya Fujita

2.*   Index to the NSSP Surface Network - Tetsuya Fujita

3.*   Outline of a Technique for Precise Rectification of Satellite Cloud Photographs - Tetsuya Fujita

4.*   Horizontal Structure of Mountain Winds - Henry A. Brown

5.*   An Investigation of Developmental Processes of the Wake Depression Through Excess Pressure Analysis of Nocturnal Showers - Joseph L. Goldman

6.*   Precipitation in the 1960 Flagstaff Mesometeorological Network - Kenneth A. Styber

7.**   On a Method of Single- and Dual-Image Photogrammetry of Panoramic Aerial Photographs - Tetsuya Fujita

8.   A Review of Researches on Analytical Mesometeorology - Tetsuya Fujita

9.*   Meteorological Interpretations of Convective Nephsystems Appearing in TIROS Cloud Photographs - Tetsuya Fujita, Toshimitsu Ushijima, William A. Hass, and George T. Dellert, Jr.

10.*   Study of the Development of Prefrontal Squall-Systems Using NSSP Network Data - Joseph L. Goldman

11.   Analysis of Selected Aircraft Data from NSSP Operation, 1962 - Tetsuya Fujita

12.   Study of a Long Condensation Trail Photographed by TIROS I - Toshimitsu Ushijima

13.   A Technique for Precise Analysis of Satellite Data; Volume I - Photogrammetry (Published as MSL Report No. 14) - Tetsuya Fujita

14.   Investigation of a Summer Jet Stream Using TIROS and Aerological Data - Kozo Ninomiya

15.   Outline of a Theory and Examples for Precise Analysis of Satellite Radiation Data - Tetsuya Fujita

16.   Preliminary Result of Analysis of the Cumulonimbus Cloud of April 21, 1961 - Tetsuya Fujita and James Arnold

17.   A Technique for Precise Analysis of Satellite Photographs - Tetsuya Fujita

18.*   Evaluation of Limb Darkening from TIROS III Radiation Data - S.H.H. Larsen, Tetsuya Fujita, and W.L. Fletcher

19.   Synoptic Interpretation of TIROS III Measurements of Infrared Radiation - Finn Pedersen and Tetsuya Fujita

20.*   TIROS III Measurements of Terrestrial Radiation and Reflected and Scattered Solar Radiation - S.H.H. Larsen, Tetsuya Fujita, and W.L. Fletcher

21.   On the Low-level Structure of a Squall Line - Henry A. Brown

22.*   Thunderstorms and the Low-level Jet - William D. Bonner

23.*   The Mesoanalysis of an Organized Convective System - Henry A. Brown

24.   Preliminary Radar and Photogrammetric Study of the Illinois Tornadoes of April 17 and 22, 1963 - Joseph L. Goldman and Tetsuya Fujita

25.   Use of TIROS Pictures for Studies of the Internal Structure of Tropical Storms - Tetsuya Fujita with Rectified Pictures from TIROS I Orbit 125, R/O 128 - Toshimitsu Ushijima

26.   An Experiment in the Determination of Geostrophic and Isallobaric Winds from NSSP Pressure Data - William Bonner

27.   Proposed Mechanism of Hook Echo Formation - Tetsuya Fujita with a Preliminary Mesosynoptic Analysis of Tornado Cyclone Case of May 26, 1963 - Tetsuya Fujita and Robbi Stuhmer

28.   The Decaying Stage of Hurricane Anna of July 1961 as Portrayed by TIROS Cloud Photographs and Infrared Radiation from the Top of the Storm - Tetsuya Fujita and James Arnold

29.   A Technique for Precise Analysis of Satellite Data, Volume II - Radiation Analysis, Section 6. Fixed-Position Scanning - Tetsuya Fujita

30.   Evaluation of Errors in the Graphical Rectification of Satellite Photographs - Tetsuya Fujita

31.   Tables of Scan Nadir and Horizontal Angles - William D. Bonner

32.   A Simplified Grid Technique for Determining Scan Lines Generated by the TIROS Scanning Radiometer - James E. Arnold

33.   A Study of Cumulus Clouds over the Flagstaff Research Network with the Use of U-2 Photographs - Dorothy L. Bradbury and Tetsuya Fujita

34.   The Scanning Printer and Its Application to Detailed Analysis of Satellite Radiation Data - Tetsuya Fujita

35.   Synoptic Study of Cold Air Outbreak over the Mediterranean using Satellite Photographs and Radiation Data - Aasmund Rabbe and Tetsuya Fujita

36.   Accurate Calibration of Doppler Winds for their use in the Computation of Mesoscale Wind Fields - Tetsuya Fujita

37.   Proposed Operation of Intrumented Aircraft for Research on Moisture Fronts and Wake Depressions - Tetsuya Fujita and Dorothy L. Bradbury

38.   Statistical and Kinematical Properties of the Low-level Jet Stream - William D. Bonner

39.   The Illinois Tornadoes of 17 and 22 April 1963 - Joseph L. Goldman

40.   Resolution of the Nimbus High Resolution Infrared Radiometer - Tetsuya Fujita and William R. Bandeen

41.   On the Determination of the Exchange Coefficients in Convective Clouds - Rodger A. Brown

*   Out of Print
**   To be published